

LA-UR-21-24093

Approved for public release; distribution is unlimited.

Title: Including 238U(n,f)/235U(n,f) and 239Pu(n,f)/235U(n,f) NIFFTE fissionTPC Cross-sections into the Neutron Data Standards Database

Author(s): Neudecker, Denise
Pronyaev, Vladimir G.
Snyder, Luke

Intended for: Report

Issued: 2022-05-16 (rev.2)



Los Alamos National Laboratory, an affirmative action/equal opportunity employer, is operated by Triad National Security, LLC for the National Nuclear Security Administration of U.S. Department of Energy under contract 89233218CNA00001. By approving this article, the publisher recognizes that the U.S. Government retains nonexclusive, royalty-free license to publish or reproduce the published form of this contribution, or to allow others to do so, for U.S. Government purposes. Los Alamos National Laboratory requests that the publisher identify this article as work performed under the auspices of the U.S. Department of Energy. Los Alamos National Laboratory strongly supports academic freedom and a researcher's right to publish; as an institution, however, the Laboratory does not endorse the viewpoint of a publication or guarantee its technical correctness.

Including $^{238}\text{U}(\text{n},\text{f})/^{235}\text{U}(\text{n},\text{f})$ and $^{239}\text{Pu}(\text{n},\text{f})/^{235}\text{U}(\text{n},\text{f})$ NIFFTE fissionTPC Cross-sections into the Neutron Data Standards Database

D. Neudecker^{a*}, V. Pronyaev^b, L. Snyder^c

^a Los Alamos National Laboratory, Los Alamos, New Mexico 87545, USA

^b International Atomic Energy Agency, P.O. Box 100, A-1400 Vienna, Austria (consultant)

^c Lawrence Livermore National Laboratory, Livermore, California 94550, USA

May 12, 2022

Contents

1	Introduction	3
2	Including fissionTPC Data into the NDS Database	4
2.1	Including $^{239}\text{Pu}(\text{n},\text{f})/^{235}\text{U}(\text{n},\text{f})$ Cross Sections into the CRD file	5
2.2	Including $^{238}\text{U}(\text{n},\text{f})/^{235}\text{U}(\text{n},\text{f})$ Cross Sections into the CRD file	11
2.3	Including Cross-correlations into the CRD file	12
2.4	Addition to the DATA.GMA file	13
3	Discussion	17
3.1	Impact of fissionTPC Data on NDS Evaluations	17
3.1.1	$^{239}\text{Pu}(\text{n},\text{f})/^{235}\text{U}(\text{n},\text{f})$ Cross Sections	17
3.1.2	$^{238}\text{U}(\text{n},\text{f})/^{235}\text{U}(\text{n},\text{f})$ Cross Sections	17
3.2	Should Tovesson <i>et al.</i> Data Above 13 MeV be Included into the NDS Database?	21
3.3	Should USU be Re-formulated to Account for Partially Independent Measurements?	22
3.4	Should the Procedure for Assessing Outlying Uncertainties be Adapted?	22
3.5	Future Work Needed on NDS Database	22
4	Counter-checking Results Obtained Above	23
4.1	$^{239}\text{Pu}(\text{n},\text{f})/^{235}\text{U}(\text{n},\text{f})$ Cross Sections	23
4.2	$^{238}\text{U}(\text{n},\text{f})/^{235}\text{U}(\text{n},\text{f})$ Cross Sections	24
4.3	General Remarks	24
5	Summary and Conclusions	27
A	Output Files for $^{235}\text{U}(\text{n},\text{f})$ Cross Sections	31
B	Output Files for $^{238}\text{U}(\text{n},\text{f})$ Cross Sections	34
C	Output Files for $^{239}\text{Pu}(\text{n},\text{f})$ Cross Sections	37
D	Comparison between this Evaluation and the LLNL Evaluation from May 2022 Using fissionTPC Data	40

*E-mail of author: dneudecker@lanl.gov

Abstract

The primary purpose of this report is to document how the $^{238}\text{U}/^{235}\text{U}$ and $^{239}\text{Pu}/^{235}\text{U}$ neutron-induced fission cross-section ratios, $^{238}\text{U}(\text{n},\text{f})/^{235}\text{U}(\text{n},\text{f})$ and $^{239}\text{Pu}(\text{n},\text{f})/^{235}\text{U}(\text{n},\text{f})$, respectively, measured by the NIFFTE fission Time Projection Chamber (fissionTPC) were included in the most recent database (termed GMA) underlying Neutron Data Standards (NDS) evaluations. This report shows and discusses NDS input files, and underlying assumptions regarding the uncertainty estimate and necessary for including these data. This uncertainty estimate and the resulting files were based on information provided by fissionTPC experimentalists, R.J.Casperson, N.S. Bowden, L. Snyder and K.T. Schmitt for the ^{238}U ratio, and by L. Snyder for the ^{239}Pu ratio. The fissionTPC data were included twice, by D. Neudecker and V. Pronyaev, to counter-check results and exclude possible mistakes in their inclusion. It is shown in both evaluations that including fissionTPC $^{239}\text{Pu}(\text{n},\text{f})/^{235}\text{U}(\text{n},\text{f})$ data points to a lower evaluated $^{239}\text{Pu}(\text{n},\text{f})$ cross section above 10 MeV than the currently released NDS data. This raises the question whether a part of a previous dataset by Tovesson *et al.*, that was previously rejected above 13 MeV for having low values, should be included in the NDS evaluation after all. The evaluated $^{238}\text{U}(\text{n},\text{f})$ cross section only changes significantly close to the threshold. The impact on the $^{235}\text{U}(\text{n},\text{f})$ cross section is minimal. fissionTPC data reduce evaluated uncertainties on both observables by 0–12% of the GMA evaluated uncertainties. However, the currently released NDS data contain in addition to these GMA evaluated uncertainties “Unrecognized Sources of Uncertainties” (USU) of 1.2%. It needs to be further discussed within the NDS project, whether the new fissionTPC data should also reduce USU.

Keywords: $^{238}\text{U}(\text{n},\text{f})/^{235}\text{U}(\text{n},\text{f})$, $^{239}\text{Pu}(\text{n},\text{f})/^{235}\text{U}(\text{n},\text{f})$, NIFFTE fissionTPC, Neutron Data Standards.

LA-UR-21-24093

1 Introduction

$^{238}\text{U}/^{235}\text{U}$ neutron-induced fission cross-section ratios, $^{238}\text{U}(\text{n},\text{f})/^{235}\text{U}(\text{n},\text{f})$, measured by the NIFFTE fission Time Projection Chamber (fissionTPC) [1–3] were published in Ref. [4]. In addition to that $^{239}\text{Pu}(\text{n},\text{f})/^{235}\text{U}(\text{n},\text{f})$ cross sections were measured with the same instrument; a journal publication, Ref. [5], will soon be submitted. All three of these cross sections, $^{235}\text{U}(\text{n},\text{f})$, $^{238}\text{U}(\text{n},\text{f})$, and $^{239}\text{Pu}(\text{n},\text{f})$, are evaluated as part of the Neutron Data Standards (NDS) project coordinated by the IAEA [6]. Data by the NDS projects are in turn often included in international nuclear data libraries, ENDF/B-VII.1 [7] and ENDF/B-VIII.0 [8] among them, which provide nuclear data for nuclear application calculations. Hence, the $^{238}\text{U}(\text{n},\text{f})/^{235}\text{U}(\text{n},\text{f})$ and $^{239}\text{Pu}(\text{n},\text{f})/^{235}\text{U}(\text{n},\text{f})$ fissionTPC data could possibly provide input for the NDS project and thus can aid in informing international nuclear data libraries and consequently nuclear application calculations.

This report describes how these new experimental data were included in the database underlying NDS evaluations. This document serves on the one hand as a documentation for the NDS project that they then can use to asses whether these data should be officially accepted to be part of the NDS database. On the other hand, this report is in answer to two NCSP FY21 milestone that request:

- Update ^{239}Pu fission cross section based on TPC results (from Pu-239/U-235 ratio data),
- Update ^{235}U fission cross section based on TPC Results (from Pu-239/U-235 ratio data).

In Section 2, a summary is given on how the $^{238}\text{U}(\text{n},\text{f})/^{235}\text{U}(\text{n},\text{f})$ and $^{239}\text{Pu}(\text{n},\text{f})/^{235}\text{U}(\text{n},\text{f})$ fissionTPC cross sections were included in the database underlying NDS evaluations by D. Neudecker. Assumptions made on uncertainties and correlations are documented as well as the GMA¹ input decks. A discussion is given in Section 3: The impact of fissionTPC data on the evaluated NDS results is shown in Section 3.1. Issues, that were raised by these evaluated results, are discussed, namely:

- fissionTPC $^{239}\text{Pu}(\text{n},\text{f})/^{235}\text{U}(\text{n},\text{f})$ cross sections lead to evaluated results above 10 MeV that are up to 2% lower than the corresponding 2018 NDS data. This new trend to lower evaluated values supports data by Tovesson *et al.* [10] that also reported lower values. Tovesson data were cut above 13 MeV for the 2018 NDS evaluation. It is mentioned in Section 3.2 that it might be good to discuss at the next NDS committee meeting whether Tovesson data above 13 MeV should be included after all,
- Unrecognized systematic uncertainties (USU) [11] were added to the 2018 NDS uncertainties to account for a large spread in experimental data that was not reflected in the uncertainties of the previous NDS version [12]. It is discussed in Section 3.3 that if we take the same procedure as for the 2018 NDS version on USU, then final reported uncertainties won't change at all. Arguments are given why this approach might not adequately describe the physics of this new measurement series,
- In Section 3.4 the issue is raised that outlying uncertainties are always assessed based on a previous evaluation penalizing new data with respect to existing data. Recommendations are given to update this procedure,
- Lastly, comments are given on future work needed on the NDS database in Ref. 3.5.

Section 4.1 discusses how V. Pronyaev included the data in order to counter-check the results and shows that both analyses led to the same conclusions and general trends. A summary and conclusions are provided in Sec. 5. The output files for the cross sections are given in the Appendix.

¹GMA is the name of both, the database and the code, underlying the NDS evaluations [9].

2 Including fissionTPC Data into the NDS Database

Here, it is described how both fissionTPC data sets were included by Denise Neudecker into the NDS database, GMA [9], while the Subsections below cover assumptions made for each measurement as part of this inclusion.

First of all, it should be highlighted that the data were included into the most recent version of the NDS database. That is NOT the version that provided input for ENDF/B-VIII.0 but a version that includes improved covariances for all $^{239}\text{Pu}(\text{n},\text{f})$ cross-section experimental data in GMA using a template of expected uncertainties [13]. It is not only important for the purpose of continuity to include fissionTPC data into the most current version, but also allows for a more valid assessment of impact of these data on the evaluation as uncertainties for past $^{239}\text{Pu}(\text{n},\text{f})$ experimental data were consistently quantified.

Denise Neudecker (DN) followed the following steps for including the data:

1. The data were read into **ARIADNE** [14] in order to identify individual uncertainties of fissionTPC data and approximate their reported correlation shapes to fit into **ARIADNE** and GMA correlation functions,
2. fissionTPC experimentalists provided energy uncertainties by giving a time resolution, time-of-flight (TOF) length and TOF length uncertainties, while GMA requires uncertainties relative to energy. DN used **ARIADNE** to calculate energy uncertainties from the information provided by the fissionTPC collaboration,
3. **ARIADNE** was then used to produce a CRD-formatted input file for the GMA database,
4. The CRD-formatted file of fissionTPC data was subsequently included into the most recent NDS file [13],
5. The code “datp-cmpq3” (provided by V. Pronyaev in summer 2018) was executed to produce the “DATA.GMA” file as input for the evaluation,
6. Interpolated data from the file “DAT.RES” produced by the code was compared to original data. This step is undertaken to investigate if there are any interpolation artifacts. For the $^{239}\text{Pu}/^{235}\text{U}$ data set, DN needed to move the energy of three points from 0.194 to 0.191, 0.4342 to 0.433 and 12.963 to 12.95 MeV because of such interpolation artifacts. All other data remained unchanged,
7. Outlying uncertainties were quantified as described in Ref. [13]. To this end, the following steps were undertaken:
 - Include new data from DAT.RES in DATA.GMA,
 - Run GMA with “GMA-cmpq1” (provided by V. Pronyaev in summer 2018),
 - Find and estimate outlying uncertainties with **ARIADNE**, and produce new CRD file for fissionTPC data,
 - Copy new CRD file (including now outlying uncertainties) over to GMDATA.CRD,
 - Re-run datp-cmpq3 to produce DAT.RES and put it in DATA.GMA.
8. The above steps were undertaken for both fissionTPC data sets. GMDATA.CRD are shown in Subsections 2.1 and 2.2. DATA.GMA input files are shown in 2.4,
9. Cross-correlations were added between the two data sets as described in Subsection 2.3.
10. Evaluated results were produced with GMA-cmpq1,
11. Plots are produced as shown in Section 3.

ARIADNE is DN's code [14] for experimental uncertainty quantification. Steps 4–11 are undertaken as DN learned them from V. Pronyaev in summer 2018 at the example of including the fissionTPC $^{238}\text{U}/^{235}\text{U}$ data set into the GMA database.

2.1 Including $^{239}\text{Pu}(\text{n},\text{f})/^{235}\text{U}(\text{n},\text{f})$ Cross Sections into the CRD file

It is described here how the fissionTPC $^{239}\text{Pu}(\text{n},\text{f})/^{235}\text{U}(\text{n},\text{f})$ data were included by DN into the CRD file and what approximations had to be undertaken.

First of all, L. Snyder supplied incident-neutron energies in the form of values for a lower and upper bin. ARIADNE as well as GMA need one energy value per data point. Hence, DN took the mid-point of the energy bin as this one-point energy; this was accepted by L. Snyder.

Then, one should note that while the data are reported in the CRD file as “shape” (normalization defined by GMA), the data were actually provided with a normalization determined by α -counting. The normalization procedure applied by the fissionTPC collaboration included determining the sample mass, non-uniformity of beam and sample, as well as beam overlap [5]. However, the final data are systematically off by a large amount given uncertainties on $^{239}\text{Pu}(\text{n},\text{f})$ evaluated data, namely by approximately 1.2%. fissionTPC experimentalists are aware that this is questionable; thus they recommended treating the data for now as a shape, until they validate their results. Hence, the data will be treated as shape data in GMA, and normalization uncertainties are ignored.

The statistical uncertainties, particle-identification, ^{239}Pu wrap-around background, residual detector-efficiency, impurity, energy-dependent beam-target overlap and non-uniformity uncertainties were explicitly provided by L. Snyder.

The first systematic uncertainty provided, termed in Ref. [5] “variational” uncertainty, accounts for the uncertainty obtained by spanning possible physics space in the variation of the particle-identification (PID) cuts. The originally reported correlation matrix in the left-hand side of Fig. 1 varies around slightly positive and slightly negative from 0.3–200 MeV, while it is positively correlated from 0.1–0.3 MeV. It is interesting to note that these variational correlations are closer to zero above 0.3 MeV, while the $^{238}\text{U}(\text{n},\text{f})/^{235}\text{U}(\text{n},\text{f})$ correlations for this uncertainty source are more pronounced positive above 0.3 MeV. The correlation matrix is approximated for GMA with a nearly diagonal one which approximates most of the original correlations on average.

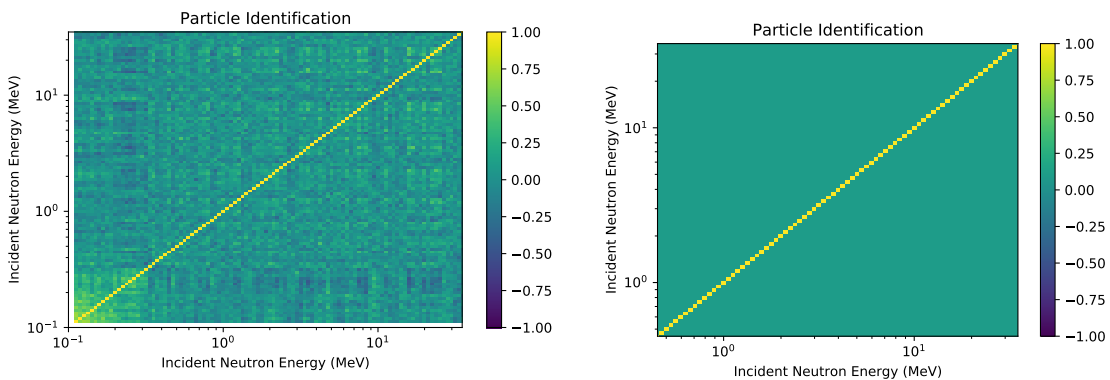


Figure 1: The correlation matrix related to uncertainties of the PID cut, as reported by the fissionTPC collaboration, is shown on the left-hand side; the approximation within the GMA database is compared on the right-hand side.

The background uncertainty accounts for background-correction uncertainties related to wrap-around of the incident beam. Backgrounds due to fission-fragment recoils and α particles are zero because the corresponding particles are clearly identified by PID cuts. The uncertainties in the variation of the PID cut is the variational uncertainty mentioned above. The shapes reported for wrap-around

correlations of both, ^{239}Pu and ^{238}U , data sets are similar although they are less strongly positive for the ^{239}Pu case. The strong correlations for this uncertainty source (Fig. 2) are approximated by an average correlation of 0.8 for GMA with the strongest correlation around the diagonal.

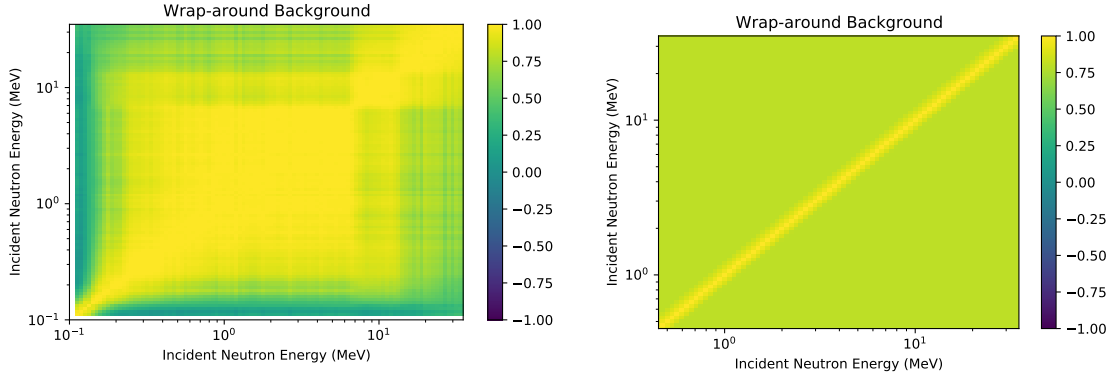


Figure 2: The correlation matrix related to uncertainties of the wrap-around background, as reported by the fissionTPC collaboration, is shown on the left-hand side; the approximation within the GMA database is compared on the right-hand side.

The residual detector-efficiency uncertainty accounts for uncertainties in the efficiency model such as in the SRIM stopping power assumption, fission-yield uncertainties, *etc.* The correlation matrix is on average diagonal in Fig. 3 with the partial correlation matrix provided by L. Snyder in private communication. Correlations to other measurements could arise because of common usage of SRIM. However, the correlation matrix is nearly diagonal to begin with, so any possible correlation would be very low. A diagonal covariance matrix is used for this uncertainty component in GMA.

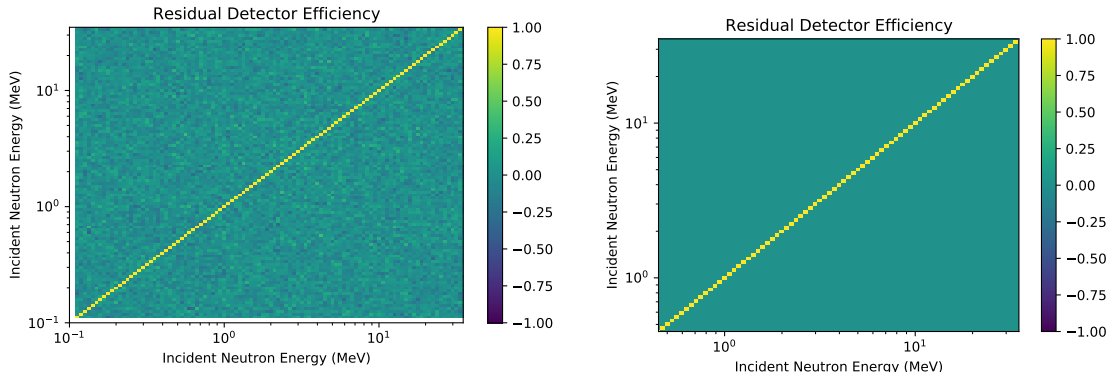


Figure 3: The correlation matrix related to uncertainties of the residual detector-efficiency correction, as reported by the fissionTPC collaboration, is shown on the left-hand side; the approximation within the GMA database is compared on the right-hand side.

The impurity uncertainty accounts for contaminations in both, ^{239}Pu and ^{235}U , samples. The impurity correlation matrix for $^{238}\text{U}(n,f)/^{235}\text{U}(n,f)$ data was fully correlated as provided by R. Casperson, while the one for $^{239}\text{Pu}(n,f)/^{235}\text{U}(n,f)$ data is closer to an average off-diagonal correlation of 0.3 as shown in Fig. 4. In the GMA entry, an average correlation of 0.35 is assumed which does not fully capture its original structure. However, the impurity uncertainty is a minor uncertainty source (0.1%) and, hence, the correlation function has little weight for total covariances in GMA.

Correlations related to beam-target overlap uncertainties are nearly diagonal in Fig. 5. One could expect these uncertainties to be fully correlated as the uncertainty source applies to the whole mea-

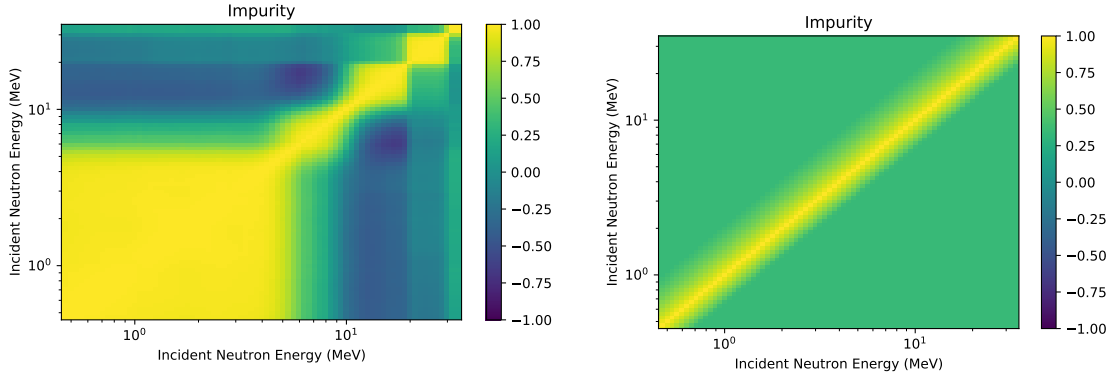


Figure 4: The correlation matrix related to impurity uncertainties, as reported by the fissionTPC collaboration, is shown on the left-hand side; the approximation within the GMA database is compared on the right-hand side.

surement, but as is pointed out in the journal article [5], the beam shape is energy-dependent and the overlap between beam and sample is measured by identifying α particles in the fissionTPC. The correlation matrix is approximated with a nearly diagonal one in GMA.

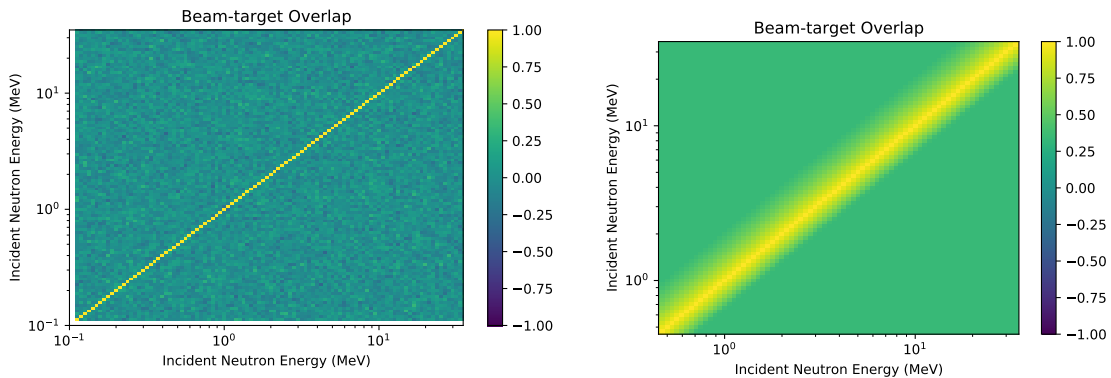


Figure 5: The correlation matrix related to beam-target overlap uncertainties, as reported by the fissionTPC collaboration, is shown on the left-hand side; the approximation within the GMA database is compared on the right-hand side.

The energy uncertainty is obtained by accounting for the TOF length uncertainty (3 mm), and the time resolution (2.75 ns full-width half maximum) which is provided in Ref. [5]. The TOF length of 8.059 m was also retrieved from the journal article. The energy uncertainties relative to the ratio data as calculated by ARIADNE from these TOF length and time resolution uncertainties are shown in Fig. 6. They are non-negligible only in those energy ranges where the cross section changes rapidly for neighboring energy bins. For the GMA CRD file, energy uncertainties are provided relative to the energy rather than the cross section. A nearly full correlation is assumed in energy space as the energy uncertainties stem from two common parameters (TOF length uncertainties and time resolution.).

L. Snyder explicitly provided attenuation-correction uncertainties. These uncertainties are rather small (at most 0.1% compared to total uncertainties from 0.8–1.8%), and hence the choice of the correlation matrix has no impact, and therefore the default is chosen. Deadtime uncertainties are zeros given the advanced data-acquisition and timing of the fissionTPC.

One caveat on the reported uncertainties is that not all parameters are varied to determine uncertainties. For instance, attenuation uncertainties did not account for uncertainties in the nuclear

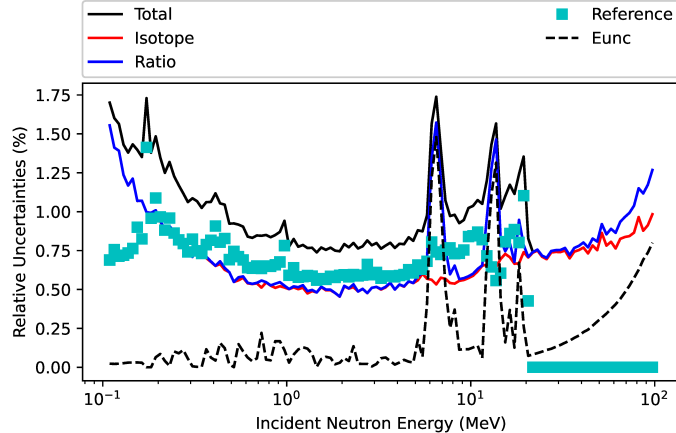


Figure 6: The total and energy uncertainties as calculated by ARIADNE are shown.

data used to calculate the attenuation correction. Also, the simulation is run independently for each energy bin for the residual detector-efficiency correction. One could obtain stronger energy-energy correlations if, for example the target thickness parameter (for fragment energy loss), was systematically biased. But there was no way of estimating how biased this, or other shared parameters, could be.

Below the CRD input deck is given including outlying uncertainties. It is shown in Fig. 6 that total uncertainties for this data set range between 0.8–1.8%. Thus the $^{239}\text{Pu}(\text{n},\text{f})/^{235}\text{U}(\text{n},\text{f})$ cross section ratios by the fissionTPC collaborations are among the most precise data in the GMA database for this particular observable.

```

60012021Pu9(n,f)/U5(n,f),SHAPE  NIFFTE TPC          J,NDS,submitted(2021)
1 4 0 1 9 119 9 8 0 0 0
UNCERTAINTIES
1 Energy Unc. calculated from 2.75ns (FWHM) and 3mm TOF length unc. (TOF length 8.059m)
3 Statistical Unc.
4 Particle Identification unc.
5 Pu-239 wrap around background unc.
6 Residual Detector Efficiency Unc.
7 Impurity Unc.
8 Beam-target overlap and non-uniformity unc.
9 Attenuation unc., dead time unc. are zero.
0.99 0.01 0.50
0.00 0.00 0.00
0.00 0.00 0.00
0.10 0.90 0.01
0.80 0.20 0.99
0.00 1.00 0.01
0.35 0.65 0.80
0.00 1.00 0.01
0.50 0.50 0.50
0.50 0.50 0.50
0.50 0.50 0.50
0 0 9 1 1 1 1 1 0 1
  0.1090  0.9979  0.2  0.0  1.2  0.5  0.4  0.2  0.1  0.7  0.1  0.0  1.7  0.0  0.0  0.0
  0.1155  0.9529  0.2  0.0  1.1  0.5  0.3  0.2  0.1  0.6  0.1  0.0  2.9  0.0  0.0  0.0
  0.1224  0.9743  0.2  0.0  1.1  0.4  0.2  0.2  0.1  0.7  0.1  0.0  3.6  0.0  0.0  0.0
  0.1296  0.9900  0.2  0.0  1.0  0.4  0.2  0.2  0.1  0.6  0.1  0.0  2.9  0.0  0.0  0.0

```

0.1373	1.0080	0.2	0.0	0.9	0.3	0.2	0.2	0.1	0.5	0.1	0.0	2.1	0.0	0.0	0.0
0.1455	1.0420	0.2	0.0	1.0	0.4	0.2	0.2	0.1	0.5	0.1	0.0	1.4	0.0	0.0	0.0
0.1540	1.0610	0.2	0.0	0.8	0.3	0.2	0.2	0.1	0.5	0.1	0.0	0.8	0.0	0.0	0.0
0.1632	1.0580	0.2	0.0	0.8	0.3	0.2	0.2	0.1	0.6	0.1	0.0	0.6	0.0	0.0	0.0
0.1729	1.1050	0.2	0.0	0.8	0.2	0.2	0.2	0.1	0.5	0.1	0.0	0.3	0.0	0.0	0.0
0.1831	1.0910	0.2	0.0	0.7	0.3	0.1	0.2	0.1	0.5	0.1	0.0	0.5	0.0	0.0	0.0
0.1910	1.0570	0.2	0.0	0.8	0.3	0.2	0.2	0.1	0.5	0.1	0.0	1.6	0.0	0.0	0.0
0.2054	1.1280	0.2	0.0	0.7	0.2	0.1	0.2	0.1	0.5	0.1	0.0	0.9	0.0	0.0	0.0
0.2175	1.1490	0.2	0.0	0.7	0.3	0.1	0.2	0.1	0.4	0.1	0.0	0.2	0.0	0.0	0.0
0.2305	1.1740	0.2	0.0	0.6	0.3	0.1	0.2	0.1	0.5	0.1	0.0	0.0	0.0	0.0	0.0
0.2442	1.1810	0.2	0.0	0.6	0.3	0.1	0.2	0.1	0.5	0.1	0.0	0.0	0.0	0.0	0.0
0.2586	1.2200	0.2	0.0	0.6	0.3	0.1	0.2	0.1	0.4	0.1	0.0	0.0	0.0	0.0	0.0
0.2740	1.2520	0.2	0.0	0.6	0.2	0.1	0.2	0.1	0.4	0.1	0.0	0.0	0.0	0.0	0.0
0.2902	1.2730	0.2	0.0	0.6	0.2	0.1	0.2	0.0	0.4	0.1	0.0	0.0	0.0	0.0	0.0
0.3074	1.2600	0.2	0.0	0.5	0.2	0.1	0.2	0.0	0.3	0.1	0.0	0.0	0.0	0.0	0.0
0.3256	1.2720	0.2	0.0	0.5	0.3	0.1	0.2	0.1	0.4	0.1	0.0	0.0	0.0	0.0	0.0
0.3449	1.2820	0.2	0.0	0.5	0.2	0.1	0.2	0.0	0.4	0.1	0.0	0.0	0.0	0.0	0.0
0.3653	1.2750	0.3	0.0	0.5	0.2	0.1	0.2	0.0	0.4	0.1	0.0	0.0	0.0	0.0	0.0
0.3870	1.2960	0.3	0.0	0.4	0.2	0.1	0.2	0.0	0.4	0.1	0.0	0.0	0.0	0.0	0.0
0.4099	1.3050	0.3	0.0	0.4	0.2	0.1	0.2	0.0	0.3	0.1	0.0	0.0	0.0	0.0	0.0
0.4330	1.3410	0.3	0.0	0.4	0.2	0.1	0.2	0.0	0.4	0.1	0.0	0.1	0.0	0.0	0.0
0.4599	1.3750	0.3	0.0	0.4	0.2	0.1	0.2	0.0	0.3	0.1	0.0	0.6	0.0	0.0	0.0
0.4872	1.4050	0.3	0.0	0.4	0.2	0.1	0.2	0.1	0.3	0.1	0.0	0.7	0.0	0.0	0.0
0.5161	1.4190	0.3	0.0	0.4	0.2	0.1	0.2	0.1	0.2	0.1	0.0	0.3	0.0	0.0	0.0
0.5467	1.4110	0.3	0.0	0.4	0.2	0.0	0.2	0.1	0.3	0.1	0.0	0.0	0.0	0.0	0.0
0.5790	1.4390	0.3	0.0	0.4	0.2	0.0	0.2	0.1	0.3	0.1	0.0	0.0	0.0	0.0	0.0
0.6134	1.4650	0.3	0.0	0.3	0.2	0.0	0.2	0.1	0.3	0.1	0.0	0.0	0.0	0.0	0.0
0.6497	1.4550	0.3	0.0	0.3	0.2	0.0	0.2	0.1	0.3	0.1	0.0	0.0	0.0	0.0	0.0
0.6881	1.4740	0.3	0.0	0.3	0.2	0.0	0.2	0.1	0.3	0.1	0.0	0.0	0.0	0.0	0.0
0.7288	1.4980	0.4	0.0	0.3	0.2	0.0	0.2	0.0	0.3	0.1	0.0	0.0	0.0	0.0	0.0
0.7721	1.5290	0.4	0.0	0.3	0.2	0.0	0.2	0.0	0.3	0.0	0.0	0.0	0.0	0.0	0.0
0.8178	1.5450	0.4	0.0	0.3	0.2	0.0	0.2	0.1	0.3	0.1	0.0	0.0	0.0	0.0	0.0
0.8664	1.5230	0.4	0.0	0.3	0.2	0.0	0.2	0.0	0.3	0.0	0.0	0.0	0.0	0.0	0.0
0.9177	1.4720	0.4	0.0	0.3	0.2	0.0	0.2	0.0	0.3	0.0	0.0	0.0	0.0	0.0	0.0
0.9721	1.4410	0.4	0.0	0.3	0.3	0.0	0.2	0.0	0.2	0.0	0.0	0.0	0.0	0.0	0.0
1.0296	1.4520	0.4	0.0	0.3	0.2	0.0	0.2	0.0	0.2	0.0	0.0	0.0	0.0	0.0	0.0
1.0904	1.4780	0.4	0.0	0.3	0.2	0.0	0.2	0.0	0.3	0.0	0.0	0.0	0.0	0.0	0.0
1.1553	1.5060	0.4	0.0	0.3	0.2	0.0	0.2	0.0	0.2	0.0	0.0	0.0	0.0	0.0	0.0
1.2242	1.5340	0.4	0.0	0.3	0.2	0.0	0.2	0.0	0.3	0.0	0.0	0.0	0.0	0.0	0.0
1.2963	1.5680	0.5	0.0	0.3	0.2	0.0	0.2	0.0	0.2	0.0	0.0	0.0	0.0	0.0	0.0
1.3735	1.5940	0.5	0.0	0.3	0.2	0.0	0.2	0.0	0.2	0.0	0.0	0.0	0.0	0.0	0.0
1.4548	1.5840	0.5	0.0	0.3	0.2	0.0	0.2	0.0	0.2	0.0	0.0	0.0	0.0	0.0	0.0
1.5404	1.5880	0.5	0.0	0.3	0.2	0.0	0.2	0.0	0.3	0.1	0.0	0.0	0.0	0.0	0.0
1.6320	1.5760	0.5	0.0	0.3	0.2	0.0	0.2	0.0	0.2	0.0	0.0	0.0	0.0	0.0	0.0
1.7288	1.5620	0.5	0.0	0.3	0.2	0.0	0.2	0.0	0.2	0.0	0.0	0.0	0.0	0.0	0.0
1.8305	1.5660	0.5	0.0	0.3	0.2	0.0	0.2	0.0	0.2	0.1	0.0	0.0	0.0	0.0	0.0
1.9400	1.5590	0.6	0.0	0.3	0.2	0.0	0.2	0.0	0.2	0.0	0.0	0.0	0.0	0.0	0.0
2.0540	1.5560	0.6	0.0	0.3	0.3	0.0	0.2	0.0	0.3	0.0	0.0	0.0	0.0	0.0	0.0
2.1755	1.5610	0.6	0.0	0.3	0.2	0.0	0.2	0.0	0.3	0.1	0.0	0.0	0.0	0.0	0.0
2.3055	1.5540	0.6	0.0	0.3	0.2	0.0	0.2	0.0	0.3	0.0	0.0	0.0	0.0	0.0	0.0
2.4415	1.5400	0.6	0.0	0.3	0.2	0.0	0.2	0.0	0.2	0.0	0.0	0.0	0.0	0.0	0.0
2.5865	1.5420	0.6	0.0	0.3	0.2	0.0	0.2	0.0	0.2	0.0	0.0	0.0	0.0	0.0	0.0
2.7400	1.5470	0.7	0.0	0.3	0.2	0.0	0.2	0.0	0.2	0.0	0.0	0.0	0.0	0.0	0.0
2.9015	1.5500	0.7	0.0	0.3	0.2	0.0	0.2	0.0	0.2	0.1	0.0	0.0	0.0	0.0	0.0
3.0735	1.5570	0.7	0.0	0.3	0.2	0.0	0.2	0.0	0.3	0.0	0.0	0.0	0.0	0.0	0.0
3.2555	1.5710	0.7	0.0	0.3	0.2	0.0	0.2	0.0	0.3	0.0	0.0	0.0	0.0	0.0	0.0

3.4490	1.5670	0.7	0.0	0.3	0.3	0.0	0.2	0.0	0.3	0.0	0.0	0.0	0.0	0.0	0.0	0.0	0.0
3.6530	1.5700	0.8	0.0	0.3	0.2	0.0	0.2	0.0	0.3	0.0	0.0	0.0	0.0	0.0	0.0	0.0	0.0
3.8695	1.5600	0.8	0.0	0.3	0.2	0.0	0.2	0.0	0.3	0.0	0.0	0.0	0.0	0.0	0.0	0.0	0.0
4.0990	1.5880	0.8	0.0	0.3	0.2	0.0	0.2	0.0	0.3	0.0	0.0	0.0	0.0	0.0	0.0	0.0	0.0
4.3420	1.5860	0.8	0.0	0.3	0.2	0.0	0.2	0.0	0.2	0.0	0.0	0.0	0.0	0.0	0.0	0.0	0.0
4.5995	1.5880	0.9	0.0	0.3	0.2	0.0	0.2	0.0	0.3	0.0	0.0	0.0	0.0	0.0	0.0	0.0	0.0
4.8720	1.5980	0.9	0.0	0.3	0.2	0.0	0.2	0.0	0.3	0.0	0.0	0.0	0.0	0.0	0.0	0.0	0.0
5.1605	1.5980	0.9	0.0	0.3	0.2	0.0	0.2	0.0	0.3	0.0	0.0	0.0	0.0	0.0	0.0	0.0	0.0
5.4665	1.6260	0.9	0.0	0.3	0.2	0.0	0.2	0.0	0.4	0.0	0.0	0.0	0.0	0.0	0.0	0.0	0.0
5.7895	1.6540	1.0	0.0	0.4	0.2	0.0	0.2	0.0	0.3	0.0	0.0	0.0	0.0	0.0	0.0	0.0	0.0
6.1335	1.5940	1.0	0.0	0.3	0.2	0.0	0.2	0.0	0.3	0.0	0.0	0.0	0.0	0.0	0.0	0.0	0.0
6.4970	1.4860	1.0	0.0	0.3	0.2	0.0	0.2	0.0	0.3	0.0	0.0	0.0	0.0	0.0	0.0	0.0	0.0
6.8810	1.3950	1.1	0.0	0.3	0.2	0.0	0.2	0.0	0.3	0.0	0.0	0.0	0.0	0.0	0.0	0.0	0.0
7.2885	1.3330	1.1	0.0	0.3	0.3	0.0	0.2	0.0	0.3	0.1	0.0	0.0	0.0	0.0	0.0	0.0	0.0
7.7210	1.3090	1.1	0.0	0.3	0.2	0.0	0.2	0.0	0.3	0.1	0.0	0.0	0.0	0.0	0.0	0.0	0.0
8.1785	1.2920	1.1	0.0	0.3	0.3	0.0	0.2	0.0	0.3	0.1	0.0	0.0	0.0	0.0	0.0	0.0	0.0
8.6635	1.2960	1.2	0.0	0.3	0.2	0.0	0.2	0.0	0.3	0.1	0.0	0.0	0.0	0.0	0.0	0.0	0.0
9.1770	1.2940	1.2	0.0	0.4	0.2	0.0	0.2	0.0	0.3	0.1	0.0	0.0	0.0	0.0	0.0	0.0	0.0
9.7205	1.3070	1.3	0.0	0.4	0.2	0.0	0.2	0.0	0.3	0.1	0.0	0.0	0.0	0.0	0.0	0.0	0.0
10.2965	1.3130	1.3	0.0	0.4	0.2	0.0	0.2	0.0	0.3	0.1	0.0	0.0	0.0	0.0	0.0	0.0	0.0
10.9040	1.3270	1.3	0.0	0.4	0.3	0.0	0.2	0.0	0.3	0.1	0.0	0.0	0.0	0.0	0.0	0.0	0.0
11.5525	1.3240	1.4	0.0	0.4	0.2	0.0	0.2	0.0	0.4	0.1	0.0	0.0	0.0	0.0	0.0	0.0	0.0
12.2420	1.3070	1.4	0.0	0.4	0.2	0.0	0.2	0.0	0.4	0.1	0.0	0.1	0.0	0.0	0.0	0.0	0.0
12.9500	1.2740	1.4	0.0	0.4	0.2	0.0	0.2	0.0	0.3	0.1	0.0	0.3	0.0	0.0	0.0	0.0	0.0
13.7350	1.2140	1.5	0.0	0.4	0.2	0.0	0.2	0.0	0.3	0.1	0.0	0.7	0.0	0.0	0.0	0.0	0.0
14.5485	1.1660	1.5	0.0	0.5	0.2	0.0	0.2	0.0	0.4	0.1	0.0	0.0	0.0	0.0	0.0	0.0	0.0
15.4035	1.1360	1.6	0.0	0.5	0.3	0.0	0.2	0.0	0.4	0.1	0.0	0.0	0.0	0.0	0.0	0.0	0.0
16.3195	1.1300	1.6	0.0	0.5	0.2	0.0	0.2	0.0	0.4	0.1	0.0	0.0	0.0	0.0	0.0	0.0	0.0
17.2875	1.1480	1.7	0.0	0.5	0.2	0.0	0.2	0.0	0.3	0.1	0.0	0.0	0.0	0.0	0.0	0.0	0.0
18.3050	1.1520	1.7	0.0	0.5	0.2	0.0	0.2	0.0	0.3	0.1	0.0	0.0	0.0	0.0	0.0	0.0	0.0
19.4000	1.1640	1.8	0.0	0.5	0.3	0.0	0.2	0.0	0.4	0.1	0.0	0.0	0.0	0.0	0.0	0.0	0.0
20.5400	1.1660	1.8	0.0	0.5	0.2	0.0	0.2	0.0	0.4	0.1	0.0	0.0	0.0	0.0	0.0	0.0	0.0
21.7550	1.1380	1.9	0.0	0.5	0.3	0.0	0.2	0.0	0.4	0.1	0.0	0.0	0.0	0.0	0.0	0.0	0.0
23.0550	1.1180	1.9	0.0	0.5	0.2	0.0	0.2	0.0	0.5	0.1	0.0	0.0	0.0	0.0	0.0	0.0	0.0
24.4150	1.1070	2.0	0.0	0.5	0.3	0.0	0.2	0.0	0.4	0.1	0.0	0.0	0.0	0.0	0.0	0.0	0.0
25.8650	1.0890	2.0	0.0	0.5	0.2	0.0	0.2	0.0	0.3	0.1	0.0	0.0	0.0	0.0	0.0	0.0	0.0
27.4000	1.1110	2.1	0.0	0.5	0.2	0.0	0.2	0.0	0.4	0.1	0.0	0.0	0.0	0.0	0.0	0.0	0.0
29.0150	1.0950	2.2	0.0	0.5	0.2	0.0	0.2	0.0	0.4	0.1	0.0	0.0	0.0	0.0	0.0	0.0	0.0
30.7350	1.0940	2.2	0.0	0.5	0.2	0.0	0.2	0.0	0.4	0.1	0.0	0.0	0.0	0.0	0.0	0.0	0.0
32.5550	1.0850	2.3	0.0	0.5	0.3	0.0	0.2	0.0	0.4	0.1	0.0	0.0	0.0	0.0	0.0	0.0	0.0
34.4900	1.0900	2.4	0.0	0.5	0.2	0.0	0.2	0.0	0.3	0.1	0.0	0.0	0.0	0.0	0.0	0.0	0.0
36.5300	1.0770	2.4	0.0	0.5	0.2	0.0	0.2	0.0	0.4	0.1	0.0	0.0	0.0	0.0	0.0	0.0	0.0
38.6950	1.0890	2.5	0.0	0.5	0.3	0.0	0.2	0.0	0.4	0.1	0.0	0.0	0.0	0.0	0.0	0.0	0.0
40.9900	1.0690	2.6	0.0	0.5	0.2	0.0	0.2	0.0	0.4	0.1	0.0	0.0	0.0	0.0	0.0	0.0	0.0
43.4200	1.0900	2.6	0.0	0.5	0.2	0.0	0.2	0.0	0.4	0.1	0.0	0.0	0.0	0.0	0.0	0.0	0.0
45.9950	1.0750	2.7	0.0	0.5	0.2	0.0	0.2	0.0	0.5	0.1	0.0	0.6	0.0	0.0	0.0	0.0	0.0
48.7200	1.0660	2.8	0.0	0.6	0.2	0.0	0.2	0.0	0.4	0.1	0.0	1.2	0.0	0.0	0.0	0.0	0.0
51.6050	1.0700	2.9	0.0	0.6	0.4	0.0	0.2	0.0	0.5	0.1	0.0	0.4	0.0	0.0	0.0	0.0	0.0
54.6650	1.0790	3.0	0.0	0.6	0.2	0.0	0.2	0.0	0.4	0.1	0.0	0.3	0.0	0.0	0.0	0.0	0.0
57.8950	1.0820	3.1	0.0	0.6	0.2	0.0	0.2	0.0	0.5	0.1	0.0	0.5	0.0	0.0	0.0	0.0	0.0
61.3350	1.0920	3.1	0.0	0.6	0.2	0.0	0.2	0.0	0.4	0.1	0.0	0.0	0.0	0.0	0.0	0.0	0.0
64.9700	1.0980	3.2	0.0	0.6	0.2	0.0	0.2	0.0	0.5	0.1	0.0	0.0	0.0	0.0	0.0	0.0	0.0
68.8100	1.0930	3.3	0.0	0.6	0.3	0.0	0.2	0.0	0.5	0.1	0.0	0.0	0.0	0.0	0.0	0.0	0.0
72.8850	1.0940	3.4	0.0	0.6	0.2	0.0	0.2	0.0	0.4	0.1	0.0	0.0	0.0	0.0	0.0	0.0	0.0
77.2100	1.0890	3.5	0.0	0.7	0.3	0.0	0.2	0.0	0.4	0.1	0.0	0.0	0.0	0.0	0.0	0.0	0.0
81.7850	1.0880	3.6	0.0	0.7	0.2	0.0	0.2	0.0	0.6	0.1	0.0	0.0	0.0	0.0	0.0	0.0	0.0

86.6350	1.0740	3.7	0.0	0.7	0.3	0.0	0.2	0.0	0.4	0.1	0.0	0.0	0.0	0.0	0.0
91.7700	1.0990	3.8	0.0	0.7	0.2	0.0	0.2	0.0	0.5	0.1	0.0	0.0	0.0	0.0	0.0
97.2050	1.1030	4.0	0.0	0.7	0.3	0.0	0.2	0.0	0.5	0.1	0.0	0.0	0.0	0.0	0.0

2.2 Including $^{238}\text{U}(\text{n},\text{f})/^{235}\text{U}(\text{n},\text{f})$ Cross Sections into the CRD file

The choices and assumptions on the $^{238}\text{U}(\text{n},\text{f})/^{235}\text{U}(\text{n},\text{f})$ cross sections were already detailed in Ref. [15] and won't be repeated here. Below the CRD input file is given that was prepared in summer 2018 by D. Neudecker and V. Pronyaev.

```

60002018U8(n,f)/U5(n,f)           NIFFTE TPC           J,PRC,97,034618(2018)
1 4 0 0 8 72 10 8 0 0 0
UNCERTAINTIES
1 Energy Uncertainty calculated from 2.03 ns and 3 mm TOF length unc. (TOF length 8.059 m)
3 Statistical Unc.
4 Particle Identification unc.
5 Pu-239 wrap around background unc.
6 Residual Detector Efficiency Unc.
7 Impurity Unc.
8 Outlying Unc. only added to DAT.GMA file.
0.99 0.01 0.50
0.00 0.00 0.00
0.00 0.00 0.00
0.50 0.50 0.50
0.99 0.01 0.50
0.00 0.00 0.00
0.99 0.01 0.50
0.50 0.50 0.50
0.50 0.50 0.50
0.50 0.50 0.50
0.50 0.50 0.50
0.50 0.50 0.50
0 0 9 1 1 1 0 0 0 0
  0.5160  0.2252  0.0  0.0 49.7  9.3 33.0  1.2 59.8  0.0  0.0  0.0  0.0  0.0  0.0  0.0
  0.5465  0.2311  0.0  0.0 48.3  5.7 31.4  1.1 61.4  0.0  0.0  0.0  0.0  0.0  0.0  0.0
  0.5790  0.2371  0.0  0.0 59.4  5.9 39.7  1.0 73.8  0.0  0.0  0.0  0.0  0.0  0.0  0.0
  0.6135  0.2434  0.0  0.0 43.5  4.5 26.8  0.9 60.9  0.0  0.0  0.0  0.0  0.0  0.0  0.0
  0.6495  0.2498  0.0  0.0 20.7  4.5 11.0  0.9 32.4  0.0  0.0  0.0  0.0  0.0  0.0  0.0
  0.6880  0.2565  0.0  0.0 19.1  1.9 9.6  0.8 29.9  0.0  0.0  0.0  0.0  0.0  0.0  0.0
  0.7290  0.2634  0.0  0.0 16.6  1.4 7.9  0.8 26.3  0.0  0.0  0.0  0.0  0.0  0.0  0.0
  0.7720  0.2704  0.0  0.0 14.8  1.3 6.9  0.7 23.8  0.0  0.0  0.0  0.0  0.0  0.0  0.0
  0.8175  0.2777  0.0  0.0 9.7  1.1 4.0  0.7 15.5  0.0  0.0  0.0  0.0  0.0  0.0  0.0
  0.8660  0.2852  0.0  0.0 6.8  0.9 2.4  0.7 10.2  0.0  0.0  0.0  0.0  0.0  0.0  0.0
  0.9175  0.2930  0.0  0.0 4.6  0.5 1.4  0.4 6.2  0.0  0.0  0.0  0.0  0.0  0.0  0.0
  0.9720  0.3011  0.0  0.0 4.4  0.2 1.2  0.5 5.9  0.0  0.0  0.0  0.0  0.0  0.0  0.0
  1.0295  0.3093  0.0  0.0 4.4  0.5 1.2  0.4 6.0  0.0  0.0  0.0  0.0  0.0  0.0  0.0
  1.0905  0.3178  0.0  0.0 3.4  0.2 0.8  0.4 4.0  0.0  0.0  0.0  0.0  0.0  0.0  0.0
  1.1555  0.3267  0.0  0.0 2.7  0.2 0.5  0.4 2.8  0.0  0.0  0.0  0.0  0.0  0.0  0.0
  1.2240  0.3357  0.0  0.0 2.5  0.3 0.5  0.3 2.5  0.0  0.0  0.0  0.0  0.0  0.0  0.0
  1.2965  0.3450  0.1  0.0 2.0  0.1 0.3  0.3 1.6  0.0  0.0  0.0  0.0  0.0  0.0  0.0
  1.3735  0.3547  0.1  0.0 1.4  0.1 0.2  0.2 0.8  0.0  0.0  0.0  0.0  0.0  0.0  0.0
  1.4545  0.3645  0.2  0.0 1.0  0.2 0.2  0.2 0.4  0.0  0.0  0.0  0.0  0.0  0.0  0.0
  1.5405  0.3747  0.3  0.0 0.9  0.1 0.2  0.1 0.3  0.0  0.0  0.0  0.0  0.0  0.0  0.0
  1.6320  0.3853  0.3  0.0 0.9  0.1 0.2  0.1 0.3  0.0  0.0  0.0  0.0  0.0  0.0  0.0
  1.7285  0.3961  0.4  0.0 0.9  0.1 0.2  0.2 0.3  0.0  0.0  0.0  0.0  0.0  0.0  0.0
  1.8310  0.4072  0.4  0.0 0.8  0.1 0.1  0.1 0.2  0.0  0.0  0.0  0.0  0.0  0.0  0.0
  1.9395  0.4187  0.4  0.0 0.8  0.1 0.1  0.1 0.2  0.0  0.0  0.0  0.0  0.0  0.0  0.0

```

EBEBEBEBEBEB
9999999999

2.3 Including Cross-correlations into the CRD file

Although the two data sets are from the same collaboration only few uncertainties are listed as correlated. The reason lies in that many of the correlation matrices are diagonal to begin with for the same observable. For instance, beam-target overlap and residual detector-efficiency uncertainties are

diagonal for the ^{239}Pu data set. Impurity uncertainties, on the other hand, are that small (maximally 0.1% for the ^{239}Pu data set) that a correlation matrix between the two data sets would have negligible, if at all, impact on the evaluation.

Hence, the remaining terms that could have correlated uncertainties are those related to PID cuts and wrap-around background. PID cut uncertainties for the ^{239}Pu data set are nearly diagonal; hence, a very low correlation coefficient of 0.1 was chosen between the two fissionTPC data sets. The only substantial source of correlated uncertainties across the two data sets was the wrap-around background that was corrected in the same fashion for both measurements. A correlation factor of 0.7 was assumed. The CRD input is given below.

2.4 Addition to the DATA.GMA file

Below the resulting DATA.GMA file from implementing the data into the CRD file and running datp-cmpq3 is given for the sake of completeness and reproducibility.

BLCK 0 0
 DATA 6000 4 0 2 10 8 0 0
 2018 1 ONIFFTE TPC J,PRC,97,034618(2018)

0.99 0.01 0.50 1
 0.00 0.00 0.00 0
 0.00 0.00 0.00 9
 0.50 0.50 0.50 1
 0.99 0.01 0.50 1
 0.00 0.00 0.00 0
 0.99 0.01 0.50 1
 0.50 0.50 0.50 0
 0.50 0.50 0.50 0
 0.50 0.50 0.50 0
 0.50 0.50 0.50 1

0.5200E+000.1018E-02 0.2 0.0 49.7 9.3 33.0 1.2 59.8 0.0 0.0 0.0 0.0 0.0 0.0
 0.5400E+000.9858E-03 0.2 0.0 48.3 5.7 31.4 1.1 61.4 0.0 0.0 0.0 0.0 0.0 0.0
 0.5700E+000.9479E-03 0.2 0.0 59.4 5.9 39.7 1.0 73.8 0.0 0.0 0.0 0.0 0.0 0.0
 0.6000E+000.9103E-03 0.2 0.0 43.5 4.5 26.8 0.9 60.9 0.0 0.0 0.0 0.0 0.0 0.0
 0.7000E+000.3120E-02 0.3 0.0 19.1 1.9 9.6 0.8 29.9 0.0 0.0 0.0 0.0 74.1 0.0
 0.7500E+000.3282E-02 0.3 0.0 11.0 1.3 7.4 0.8 25.0 0.0 0.0 0.0 0.0 23.7 0.0
 0.8000E+000.5054E-02 0.3 0.0 9.7 1.1 4.0 0.7 15.5 0.0 0.0 0.0 0.0 19.6 0.0
 0.8500E+000.7546E-02 0.3 0.0 6.8 0.9 2.4 0.7 10.2 0.0 0.0 0.0 0.0 17.0 0.0
 0.9000E+000.1407E-01 0.3 0.0 4.6 0.5 1.4 0.4 6.2 0.0 0.0 0.0 0.0 10.6 0.0
 0.9800E+000.1559E-01 0.3 0.0 4.4 0.2 1.2 0.5 5.9 0.0 0.0 0.0 0.0 13.0 0.0
 0.1000E+010.1144E-01 0.3 0.0 4.4 0.5 1.2 0.4 6.0 0.0 0.0 0.0 0.0 0.0 0.0
 0.1100E+010.2738E-01 0.3 0.0 2.1 0.2 0.6 0.4 3.4 0.0 0.0 0.0 0.0 0.0 0.0
 0.1250E+010.2635E-01 0.3 0.0 1.6 0.2 0.4 0.3 2.0 0.0 0.0 0.0 0.0 17.0 0.0
 0.1400E+010.1615E+00 0.4 0.0 0.8 0.2 0.2 0.2 0.6 0.0 0.0 0.0 0.0 3.4 0.0
 0.1600E+010.3313E+00 0.4 0.0 0.6 0.1 0.2 0.1 0.3 0.0 0.0 0.0 0.0 0.0 0.0
 0.1800E+010.3751E+00 0.4 0.0 0.6 0.1 0.2 0.2 0.2 0.0 0.0 0.0 0.0 0.0 0.0
 0.2000E+010.4098E+00 0.4 0.0 0.6 0.1 0.1 0.1 0.2 0.0 0.0 0.0 0.0 0.0 0.0
 0.2200E+010.4226E+00 0.4 0.0 0.8 0.1 0.1 0.1 0.2 0.0 0.0 0.0 0.0 0.0 0.0
 0.2400E+010.4199E+00 0.5 0.0 0.6 0.1 0.1 0.1 0.2 0.0 0.0 0.0 0.0 0.0 0.0
 0.2600E+010.4159E+00 0.5 0.0 0.8 0.1 0.1 0.1 0.2 0.0 0.0 0.0 0.0 0.0 1.5
 0.2800E+010.4327E+00 0.5 0.0 0.8 0.1 0.1 0.1 0.2 0.0 0.0 0.0 0.0 0.0 0.0
 0.3000E+010.4222E+00 0.5 0.0 0.5 0.1 0.1 0.1 0.2 0.0 0.0 0.0 0.0 0.0 0.0

0.3600E+010.4597E+00	0.6	0.0	0.6	0.1	0.1	0.1	0.2	0.0	0.0	0.0	0.0	0.0	0.0	0.0	0.0
0.4000E+010.4802E+00	0.6	0.0	0.6	0.1	0.1	0.1	0.2	0.0	0.0	0.0	0.0	0.0	0.0	0.0	0.0
0.4500E+010.4967E+00	0.6	0.0	0.6	0.1	0.1	0.1	0.2	0.0	0.0	0.0	0.0	0.0	0.0	0.0	0.0
0.5000E+010.5056E+00	0.7	0.0	0.9	0.1	0.1	0.1	0.2	0.0	0.0	0.0	0.0	0.0	0.0	0.0	0.0
0.5300E+010.5258E+00	0.7	0.0	0.9	0.1	0.1	0.1	0.2	0.0	0.0	0.0	2.2	0.0			
0.5500E+010.5200E+00	0.7	0.0	0.9	0.1	0.1	0.1	0.2	0.0	0.0	0.0	0.0	0.0	0.0	0.0	0.0
0.5800E+010.5407E+00	0.7	0.0	1.0	0.2	0.1	0.1	0.2	0.0	0.0	0.0	0.0	0.0	0.0	0.0	0.0
0.6200E+010.5713E+00	0.7	0.0	0.9	0.1	0.1	0.1	0.2	0.0	0.0	0.0	0.0	0.0	0.0	0.0	0.0
0.6500E+010.5894E+00	0.8	0.0	0.9	0.1	0.1	0.1	0.2	0.0	0.0	0.0	1.8	0.0			
0.7000E+010.6133E+00	0.8	0.0	0.8	0.1	0.1	0.1	0.1	0.0	0.0	0.0	1.7	0.0			
0.7500E+010.5849E+00	0.8	0.0	0.8	0.0	0.1	0.1	0.2	0.0	0.0	0.0	1.5	0.0			
0.7750E+010.5727E+00	0.8	0.0	0.8	0.1	0.1	0.1	0.2	0.0	0.0	0.0	0.0	0.0	0.0	0.0	0.0
0.8000E+010.5664E+00	0.8	0.0	0.9	0.0	0.1	0.1	0.2	0.0	0.0	0.0	0.0	0.0	0.0	0.0	0.0
0.8500E+010.5533E+00	0.9	0.0	0.9	0.0	0.1	0.1	0.2	0.0	0.0	0.0	0.0	0.0	0.0	0.0	0.0
0.9000E+010.5616E+00	0.9	0.0	0.9	0.1	0.1	0.1	0.2	0.0	0.0	0.0	0.0	0.0	0.0	0.0	0.0
0.1000E+020.5673E+00	0.9	0.0	0.6	0.2	0.1	0.1	0.2	0.0	0.0	0.0	0.0	0.0	0.0	0.0	0.0
0.1100E+020.5757E+00	1.0	0.0	1.0	0.1	0.1	0.1	0.2	0.0	0.0	0.0	0.0	0.0	0.0	0.0	0.0
0.1150E+020.5831E+00	1.0	0.0	1.0	0.1	0.1	0.1	0.2	0.0	0.0	0.0	0.0	0.0	0.0	0.0	0.0
0.1200E+020.5720E+00	1.0	0.0	1.1	0.1	0.1	0.2	0.2	0.0	0.0	0.0	0.0	0.0	0.0	0.0	0.0
0.1300E+020.5420E+00	1.1	0.0	1.1	0.1	0.1	0.1	0.2	0.0	0.0	0.0	0.0	0.0	0.0	0.0	0.0
0.1400E+020.5472E+00	1.1	0.0	1.1	0.1	0.1	0.1	0.2	0.0	0.0	0.0	0.0	0.0	0.0	0.0	0.0
0.1450E+020.5647E+00	1.1	0.0	1.1	0.1	0.1	0.1	0.2	0.0	0.0	0.0	0.0	0.0	0.0	0.0	0.0
0.1500E+020.5731E+00	1.2	0.0	1.0	0.1	0.1	0.1	0.2	0.0	0.0	0.0	0.0	0.0	0.0	0.0	0.0
0.1600E+020.6064E+00	1.2	0.0	1.1	0.0	0.1	0.1	0.2	0.0	0.0	0.0	0.0	0.0	0.0	0.0	0.0
0.1700E+020.6294E+00	1.2	0.0	1.1	0.0	0.1	0.2	0.1	0.0	0.0	0.0	0.0	0.0	0.0	0.0	0.0
0.1800E+020.6410E+00	1.3	0.0	1.1	0.2	0.1	0.1	0.1	0.0	0.0	0.0	0.0	0.0	0.0	0.0	0.0
0.1900E+020.6669E+00	1.3	0.0	1.1	0.1	0.1	0.1	0.1	0.0	0.0	0.0	0.0	0.0	0.0	0.0	0.0
0.2100E+020.7251E+00	1.3	0.0	1.1	0.1	0.1	0.1	0.1	0.0	0.0	0.0	0.0	0.0	0.0	0.0	0.0
0.2200E+020.7363E+00	1.4	0.0	1.1	0.1	0.1	0.1	0.1	0.0	0.0	0.0	0.0	0.0	0.0	0.0	0.0
0.2300E+020.7467E+00	1.4	0.0	1.1	0.1	0.1	0.1	0.1	0.0	0.0	0.0	0.0	0.0	0.0	0.0	0.0
0.2400E+020.7291E+00	1.5	0.0	1.1	0.1	0.1	0.1	0.1	0.0	0.0	0.0	0.0	0.0	0.0	0.0	0.0
0.2600E+020.7443E+00	1.5	0.0	1.1	0.1	0.1	0.1	0.1	0.0	0.0	0.0	0.0	0.0	0.0	0.0	0.0
0.2700E+020.7367E+00	1.6	0.0	1.1	0.2	0.1	0.2	0.1	0.0	0.0	0.0	0.0	0.0	0.0	0.0	0.0
0.2900E+020.7498E+00	1.6	0.0	1.1	0.0	0.1	0.1	0.1	0.0	0.0	0.0	0.0	0.0	0.0	0.0	0.0
0.3000E+020.7583E+00	1.6	0.0	1.1	0.1	0.1	0.1	0.1	0.0	0.0	0.0	0.0	0.0	0.0	0.0	0.0
0.0000E+000.0000E+00	0.0	0.0	0.0	0.0	0.0	0.0	0.0	0.0	0.0	0.0	0.0	0.0	0.0	0.0	0.0

DATA 6001 4 0 2 9 8 0 0

J,NDS,submitted(2021

0.99	0.01	0.50	0
0.00	0.00	0.00	0
0.00	0.00	0.00	9
0.10	0.90	0.01	1
0.80	0.20	0.99	1
0.00	1.00	0.01	1
0.35	0.65	0.80	1
0.00	1.00	0.01	1
0.50	0.50	0.50	1
0.50	0.50	0.50	0
0.50	0.50	0.50	0

6000	14	14	15	15	0	0	0	0	0	0	0	0	0	0	0
------	----	----	----	----	---	---	---	---	---	---	---	---	---	---	---

0.1	0.7	0.0	0.0	0.0	0.0	0.0	0.0	0.0	0.0	0.0	0.0	0.0	0.0	0.0	0.0
-----	-----	-----	-----	-----	-----	-----	-----	-----	-----	-----	-----	-----	-----	-----	-----

0.1000E+000.9852E+00	0.2	0.0	1.2	0.5	0.4	0.2	0.1	0.7	0.1	0.0	1.7	0.0			
0.1200E+000.9690E+00	0.2	0.0	0.6	0.4	0.2	0.2	0.1	0.6	0.1	0.0	3.1	0.0			
0.1500E+000.1049E+01	0.2	0.0	0.5	0.3	0.2	0.2	0.1	0.5	0.1	0.0	1.4	0.0			
0.1700E+000.1089E+01	0.2	0.0	0.6	0.2	0.2	0.2	0.1	0.6	0.1	0.0	0.5	0.0			
0.1800E+000.1091E+01	0.2	0.0	0.7	0.3	0.1	0.2	0.1	0.5	0.1	0.0	0.5	0.0			

0.1900E+000.1053E+01	0.2	0.0	0.8	0.3	0.2	0.2	0.1	0.5	0.1	0.0	1.6	0.0
0.2100E+000.1142E+01	0.2	0.0	0.7	0.2	0.1	0.2	0.1	0.5	0.1	0.0	0.9	0.0
0.2200E+000.1148E+01	0.2	0.0	0.7	0.3	0.1	0.2	0.1	0.4	0.1	0.0	0.2	0.0
0.2300E+000.1176E+01	0.2	0.0	0.6	0.3	0.1	0.2	0.1	0.5	0.1	0.0	0.0	0.0
0.2450E+000.1185E+01	0.2	0.0	0.6	0.3	0.1	0.2	0.1	0.5	0.1	0.0	0.0	0.0
0.2600E+000.1223E+01	0.2	0.0	0.6	0.3	0.1	0.2	0.1	0.4	0.1	0.0	0.0	0.0
0.2700E+000.1232E+01	0.2	0.0	0.6	0.2	0.1	0.2	0.1	0.4	0.1	0.0	0.0	0.0
0.3000E+000.1262E+01	0.2	0.0	0.4	0.2	0.1	0.2	0.0	0.4	0.1	0.0	0.0	0.0
0.3250E+000.1272E+01	0.2	0.0	0.5	0.3	0.1	0.2	0.1	0.4	0.1	0.0	0.0	0.0
0.3500E+000.1283E+01	0.2	0.0	0.5	0.2	0.1	0.2	0.0	0.4	0.1	0.0	0.0	0.0
0.3750E+000.1282E+01	0.3	0.0	0.3	0.2	0.1	0.2	0.0	0.4	0.1	0.0	0.0	0.0
0.4000E+000.1319E+01	0.3	0.0	0.4	0.2	0.1	0.2	0.0	0.3	0.1	0.0	0.0	0.0
0.4250E+000.1317E+01	0.3	0.0	0.4	0.2	0.1	0.2	0.0	0.4	0.1	0.0	0.1	0.0
0.4500E+000.1363E+01	0.3	0.0	0.4	0.2	0.1	0.2	0.0	0.3	0.1	0.0	0.6	0.0
0.4750E+000.1410E+01	0.3	0.0	0.4	0.2	0.1	0.2	0.1	0.3	0.1	0.0	0.7	0.0
0.5200E+000.1416E+01	0.3	0.0	0.4	0.2	0.1	0.2	0.1	0.2	0.1	0.0	0.3	0.0
0.5400E+000.1412E+01	0.3	0.0	0.4	0.2	0.0	0.2	0.1	0.3	0.1	0.0	0.0	0.0
0.5700E+000.1426E+01	0.3	0.0	0.4	0.2	0.0	0.2	0.1	0.3	0.1	0.0	0.0	0.0
0.6000E+000.1462E+01	0.3	0.0	0.3	0.2	0.0	0.2	0.1	0.3	0.1	0.0	0.0	0.0
0.6500E+000.1455E+01	0.3	0.0	0.3	0.2	0.0	0.2	0.1	0.3	0.1	0.0	0.0	0.0
0.7000E+000.1477E+01	0.3	0.0	0.3	0.2	0.0	0.2	0.1	0.3	0.1	0.0	0.0	0.0
0.7500E+000.1513E+01	0.4	0.0	0.2	0.2	0.0	0.2	0.0	0.3	0.1	0.0	0.0	0.0
0.8000E+000.1553E+01	0.4	0.0	0.3	0.2	0.0	0.2	0.1	0.3	0.1	0.0	0.0	0.0
0.8500E+000.1539E+01	0.4	0.0	0.3	0.2	0.0	0.2	0.0	0.3	0.0	0.0	0.0	0.0
0.9000E+000.1484E+01	0.4	0.0	0.3	0.2	0.0	0.2	0.0	0.3	0.0	0.0	0.0	0.0
0.9800E+000.1435E+01	0.4	0.0	0.3	0.3	0.0	0.2	0.0	0.2	0.0	0.0	0.0	0.0
0.1000E+010.1447E+01	0.4	0.0	0.3	0.2	0.0	0.2	0.0	0.2	0.0	0.0	0.0	0.0
0.1100E+010.1482E+01	0.4	0.0	0.2	0.2	0.0	0.2	0.0	0.2	0.0	0.0	0.0	0.0
0.1250E+010.1550E+01	0.4	0.0	0.2	0.2	0.0	0.2	0.0	0.2	0.0	0.0	0.0	0.0
0.1400E+010.1595E+01	0.5	0.0	0.2	0.2	0.0	0.2	0.0	0.2	0.0	0.0	0.0	0.0
0.1600E+010.1581E+01	0.5	0.0	0.2	0.2	0.0	0.2	0.0	0.2	0.1	0.0	0.0	0.0
0.1800E+010.1560E+01	0.5	0.0	0.2	0.2	0.0	0.2	0.0	0.2	0.1	0.0	0.0	0.0
0.2000E+010.1557E+01	0.6	0.0	0.2	0.2	0.0	0.2	0.0	0.2	0.0	0.0	0.0	0.0
0.2200E+010.1562E+01	0.6	0.0	0.3	0.2	0.0	0.2	0.0	0.3	0.1	0.0	0.0	0.0
0.2400E+010.1541E+01	0.6	0.0	0.2	0.2	0.0	0.2	0.0	0.2	0.0	0.0	0.0	0.0
0.2600E+010.1542E+01	0.6	0.0	0.3	0.2	0.0	0.2	0.0	0.2	0.0	0.0	0.0	0.0
0.2800E+010.1549E+01	0.7	0.0	0.3	0.2	0.0	0.2	0.0	0.2	0.0	0.0	0.0	0.0
0.3000E+010.1555E+01	0.7	0.0	0.2	0.2	0.0	0.2	0.0	0.3	0.0	0.0	0.0	0.0
0.3600E+010.1572E+01	0.8	0.0	0.2	0.2	0.0	0.2	0.0	0.3	0.0	0.0	0.0	0.0
0.4000E+010.1574E+01	0.8	0.0	0.2	0.2	0.0	0.2	0.0	0.3	0.0	0.0	0.0	0.0
0.4500E+010.1585E+01	0.9	0.0	0.2	0.2	0.0	0.2	0.0	0.2	0.0	0.0	0.0	0.0
0.5000E+010.1600E+01	0.9	0.0	0.3	0.2	0.0	0.2	0.0	0.3	0.0	0.0	0.0	0.0
0.5300E+010.1605E+01	0.9	0.0	0.3	0.2	0.0	0.2	0.0	0.3	0.0	0.0	0.0	0.0
0.5500E+010.1628E+01	0.9	0.0	0.3	0.2	0.0	0.2	0.0	0.4	0.0	0.0	0.0	0.0
0.5800E+010.1655E+01	1.0	0.0	0.4	0.2	0.0	0.2	0.0	0.3	0.0	0.0	0.0	0.0
0.6200E+010.1574E+01	1.0	0.0	0.3	0.2	0.0	0.2	0.0	0.3	0.0	0.0	0.0	0.0
0.6500E+010.1485E+01	1.0	0.0	0.3	0.2	0.0	0.2	0.0	0.3	0.0	0.0	0.0	0.0
0.7000E+010.1369E+01	1.1	0.0	0.3	0.2	0.0	0.2	0.0	0.3	0.0	0.0	0.0	0.0
0.7500E+010.1311E+01	1.1	0.0	0.3	0.3	0.0	0.2	0.0	0.3	0.1	0.0	0.0	0.0
0.7750E+010.1308E+01	1.1	0.0	0.3	0.2	0.0	0.2	0.0	0.3	0.1	0.0	0.0	0.0
0.8000E+010.1301E+01	1.1	0.0	0.3	0.3	0.0	0.2	0.0	0.3	0.1	0.0	0.0	0.0
0.8500E+010.1292E+01	1.2	0.0	0.3	0.2	0.0	0.2	0.0	0.3	0.1	0.0	0.0	0.0
0.9000E+010.1292E+01	1.2	0.0	0.4	0.2	0.0	0.2	0.0	0.3	0.1	0.0	0.0	0.0
0.1000E+020.1310E+01	1.3	0.0	0.3	0.2	0.0	0.2	0.0	0.3	0.1	0.0	0.0	0.0
0.1100E+020.1328E+01	1.3	0.0	0.4	0.3	0.0	0.2	0.0	0.3	0.1	0.0	0.0	0.0
0.1150E+020.1325E+01	1.4	0.0	0.4	0.2	0.0	0.2	0.0	0.4	0.1	0.0	0.0	0.0

0.1200E+020.1322E+01	1.4	0.0	0.4	0.2	0.0	0.2	0.0	0.4	0.1	0.0	0.1	0.0
0.1300E+020.1271E+01	1.4	0.0	0.4	0.2	0.0	0.2	0.0	0.3	0.1	0.0	0.3	0.0
0.1400E+020.1194E+01	1.5	0.0	0.4	0.2	0.0	0.2	0.0	0.3	0.1	0.0	0.7	0.0
0.1450E+020.1168E+01	1.5	0.0	0.5	0.2	0.0	0.2	0.0	0.4	0.1	0.0	0.0	0.0
0.1500E+020.1140E+01	1.6	0.0	0.5	0.3	0.0	0.2	0.0	0.4	0.1	0.0	0.0	0.0
0.1600E+020.1131E+01	1.6	0.0	0.5	0.2	0.0	0.2	0.0	0.4	0.1	0.0	0.0	0.0
0.1700E+020.1145E+01	1.7	0.0	0.5	0.2	0.0	0.2	0.0	0.3	0.1	0.0	0.0	0.0
0.1800E+020.1146E+01	1.7	0.0	0.5	0.2	0.0	0.2	0.0	0.3	0.1	0.0	0.0	0.0
0.1900E+020.1159E+01	1.8	0.0	0.5	0.3	0.0	0.2	0.0	0.4	0.1	0.0	0.0	0.0
0.2100E+020.1151E+01	1.8	0.0	0.5	0.2	0.0	0.2	0.0	0.4	0.1	0.0	0.0	0.0
0.2200E+020.1136E+01	1.9	0.0	0.5	0.3	0.0	0.2	0.0	0.4	0.1	0.0	0.0	0.0
0.2300E+020.1118E+01	1.9	0.0	0.5	0.2	0.0	0.2	0.0	0.5	0.1	0.0	0.0	0.0
0.2400E+020.1107E+01	2.0	0.0	0.5	0.3	0.0	0.2	0.0	0.4	0.1	0.0	0.0	0.0
0.2600E+020.1089E+01	2.0	0.0	0.5	0.2	0.0	0.2	0.0	0.3	0.1	0.0	0.0	0.0
0.2700E+020.1112E+01	2.1	0.0	0.5	0.2	0.0	0.2	0.0	0.4	0.1	0.0	0.0	0.0
0.2900E+020.1095E+01	2.2	0.0	0.5	0.2	0.0	0.2	0.0	0.4	0.1	0.0	0.0	0.0
0.3000E+020.1096E+01	2.2	0.0	0.5	0.2	0.0	0.2	0.0	0.4	0.1	0.0	0.0	0.0
0.3200E+020.1086E+01	2.3	0.0	0.5	0.3	0.0	0.2	0.0	0.4	0.1	0.0	0.0	0.0
0.3400E+020.1090E+01	2.4	0.0	0.5	0.2	0.0	0.2	0.0	0.3	0.1	0.0	0.0	0.0
0.3600E+020.1077E+01	2.4	0.0	0.5	0.2	0.0	0.2	0.0	0.4	0.1	0.0	0.0	0.0
0.3800E+020.1089E+01	2.5	0.0	0.5	0.3	0.0	0.2	0.0	0.4	0.1	0.0	0.0	0.0
0.4000E+020.1071E+01	2.6	0.0	0.5	0.2	0.0	0.2	0.0	0.4	0.1	0.0	0.0	0.0
0.4400E+020.1090E+01	2.6	0.0	0.5	0.2	0.0	0.2	0.0	0.4	0.1	0.0	0.0	0.0
0.4600E+020.1075E+01	2.7	0.0	0.5	0.2	0.0	0.2	0.0	0.5	0.1	0.0	0.6	0.0
0.4800E+020.1066E+01	2.8	0.0	0.6	0.2	0.0	0.2	0.0	0.4	0.1	0.0	1.2	0.0
0.5200E+020.1070E+01	2.9	0.0	0.6	0.4	0.0	0.2	0.0	0.5	0.1	0.0	0.4	0.0
0.5400E+020.1078E+01	3.0	0.0	0.6	0.2	0.0	0.2	0.0	0.4	0.1	0.0	0.3	0.0
0.5800E+020.1082E+01	3.1	0.0	0.6	0.2	0.0	0.2	0.0	0.5	0.1	0.0	0.5	0.0
0.6000E+020.1093E+01	3.1	0.0	0.6	0.2	0.0	0.2	0.0	0.4	0.1	0.0	0.0	0.0
0.6400E+020.1098E+01	3.2	0.0	0.6	0.2	0.0	0.2	0.0	0.5	0.1	0.0	0.0	0.0
0.6800E+020.1093E+01	3.3	0.0	0.6	0.3	0.0	0.2	0.0	0.5	0.1	0.0	0.0	0.0
0.7200E+020.1095E+01	3.4	0.0	0.6	0.2	0.0	0.2	0.0	0.4	0.1	0.0	0.0	0.0
0.7600E+020.1088E+01	3.5	0.0	0.7	0.3	0.0	0.2	0.0	0.4	0.1	0.0	0.0	0.0
0.8000E+020.1087E+01	3.6	0.0	0.7	0.2	0.0	0.2	0.0	0.6	0.1	0.0	0.0	0.0
0.8800E+020.1073E+01	3.7	0.0	0.7	0.3	0.0	0.2	0.0	0.4	0.1	0.0	0.0	0.0
0.9200E+020.1099E+01	3.8	0.0	0.7	0.2	0.0	0.2	0.0	0.5	0.1	0.0	0.0	0.0
0.9600E+020.1104E+01	4.0	0.0	0.7	0.3	0.0	0.2	0.0	0.5	0.1	0.0	0.0	0.0
0.0000E+000.0000E+00	0.0	0.0	0.0	0.0	0.0	0.0	0.0	0.0	0.0	0.0	0.0	0.0

EDBL 0 0

3 Discussion

3.1 Impact of fissionTPC Data on NDS Evaluations

3.1.1 $^{239}\text{Pu}(\text{n},\text{f})/^{235}\text{U}(\text{n},\text{f})$ Cross Sections

In Fig. 7, the impact of fissionTPC $^{239}\text{Pu}(\text{n},\text{f})/^{235}\text{U}(\text{n},\text{f})$ cross sections on the NDS evaluation is shown. First of all, it should be noted that the green data are the ones reported by the fissionTPC collaboration and stored in the CRD file. Contrary to that, the black data are those in the DATA.GMA file. They are interpolated to be on the grid of the NDS data and are re-normalized as the data were input as shape data. This normalization factor obtained by the GMA code was 0.9880. The important point of this comparison is two-fold: First, the interpolation procedure does not lead to artifacts (with an exception of three data points mentioned above). The second point is that, indeed, the fissionTPC data are systematically off-set by a factor of approximately 1.2% from the bulk of other data in the database that define the evaluated data, something that was already mentioned by fissionTPC experimentalists. This systematic off-set was the reason the data were treated as shape.

It can be seen from Figs. 7 and 8 that evaluated results change only modestly up to 10 MeV. It should be emphasized that we compare here the impact of fissionTPC data to an evaluation including all updates to $^{239}\text{Pu}(\text{n},\text{f})$ cross-section covariances in the CRD file according to a template of expected (n,f) measurement uncertainties [13]; this is not a comparison to the 2018 NDS version. However, we compare here two evaluations that only differ in considering the two fissionTPC data sets. Consequently, this is a clean comparison showing the impact of fissionTPC data on the current NDS file.

Large changes in the ratio cross section can be observed above 10 MeV where fissionTPC $^{239}\text{Pu}(\text{n},\text{f})/^{235}\text{U}(\text{n},\text{f})$ cross sections would indicate smaller values for this ratio than currently in ENDF/B-VIII.0. This change, albeit large with up to 2%, is still within the GMA uncertainties as can be seen from Figs. 7 and 9. In fact most of the fissionTPC data are well within the credible range of the evaluation compared to an evaluation without fissionTPC data, except for one outlier at 0.2 MeV in Fig. 9. This shows that the data from the fissionTPC collaboration validated the trend of the evaluated ratio data that results from a database of several hundreds of data. Contrary to previous data sets, however, another type of fission detector was employed for the fissionTPC measurement. While most (n,f) cross sections in GMA were measured with a traditional fission or ionization chamber, the fissionTPC project employed a time-projection chamber which allowed accurate tracking of any charged particles in three dimensions. Hence, fissionTPC data agreeing with the previous evaluation provides a validation of previous measurement techniques on average.

One might question the statement above by stating that fissionTPC data are 1.2% systematically off. However, the normalization of the data set was NOT determined with the fission time-projection chamber but by a standard techniques like α counting and α spectroscopy that have been employed for many other measurements in the GMA database. Also, the normalization is, mathematically speaking, an independent observable compared to the shape of the data set.

The fissionTPC $^{239}\text{Pu}(\text{n},\text{f})/^{235}\text{U}(\text{n},\text{f})$ cross sections lead to GMA evaluated $^{239}\text{Pu}(\text{n},\text{f})$ uncertainties that are by up to 12% lower than those obtained without these data. This reduction, however, does not consider USU uncertainties. This point will be discussed in Subsection 3.3.

While fissionTPC $^{239}\text{Pu}(\text{n},\text{f})/^{235}\text{U}(\text{n},\text{f})$ cross section contain information on both isotopes, it is shown in Fig. 8 that mostly $^{239}\text{Pu}(\text{n},\text{f})$ cross sections are impacted, while the change in $^{235}\text{U}(\text{n},\text{f})$ cross sections and uncertainties is negligible.

3.1.2 $^{238}\text{U}(\text{n},\text{f})/^{235}\text{U}(\text{n},\text{f})$ Cross Sections

In Fig. 10, the impact of fissionTPC $^{238}\text{U}(\text{n},\text{f})/^{235}\text{U}(\text{n},\text{f})$ cross sections on the NDS evaluation is shown. As for the $^{239}\text{Pu}(\text{n},\text{f})/^{235}\text{U}(\text{n},\text{f})$ ratio, the green data are the ones reported by the fissionTPC

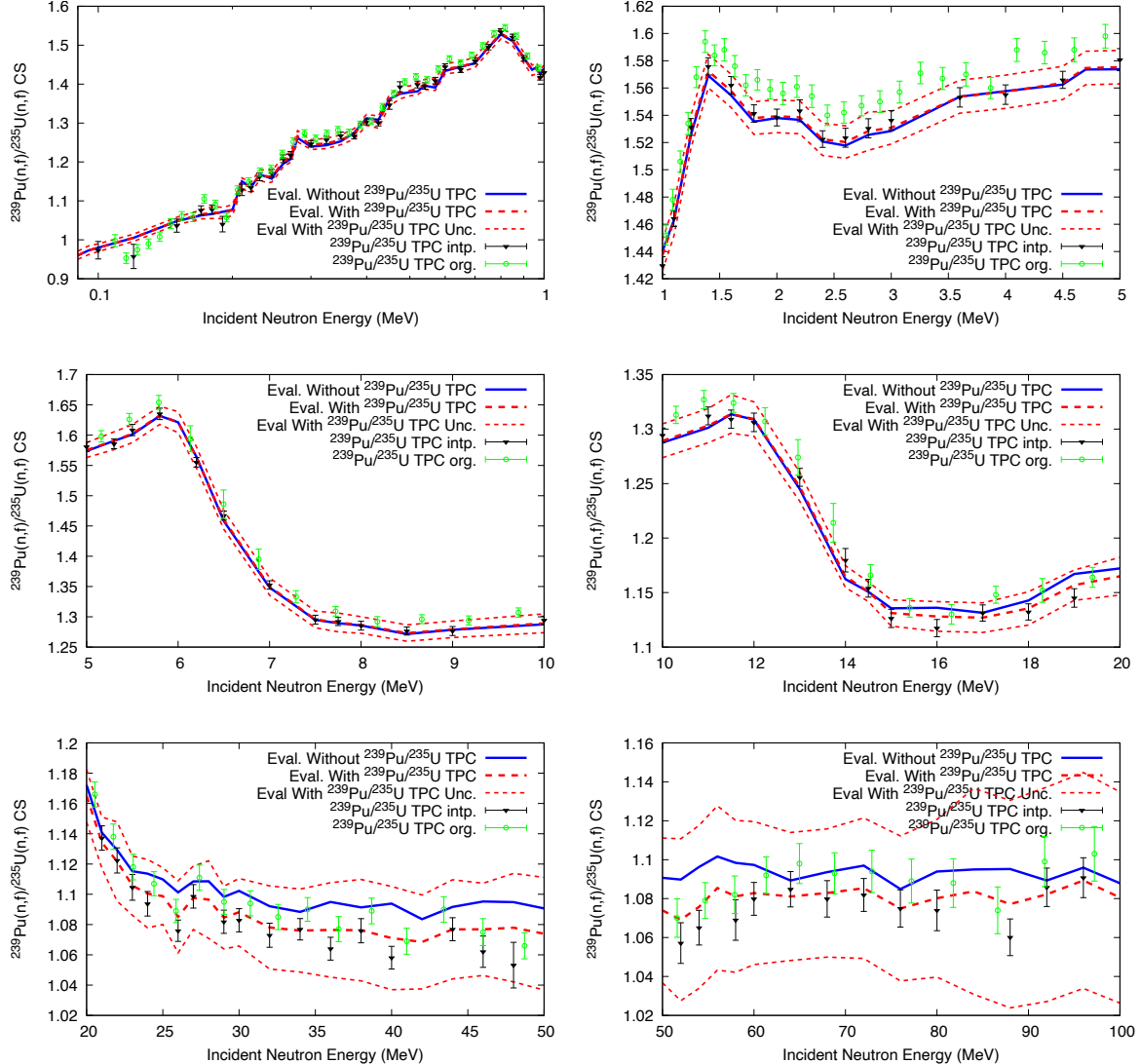


Figure 7: Evaluated $^{239}\text{Pu}(n,f)/^{235}\text{U}(n,f)$ cross sections are shown including (red thick dashed line) and excluding (blue solid line) fissionTPC data. Evaluated uncertainties including fissionTPC data are also shown in less thick red dashed lines. fissionTPC data as reported by the collaboration are shown in green, while the interpolated and renormalized data are shown in black.

collaboration and stored in the CRD file, while the black ones are those in the DATA.GMA file. The black data are interpolated to be on the grid of the NDS data and are re-normalized as the data were reported as shape data in Ref. [4]. The experimentalists normalized in Ref. [4] the ratio with respect to ENDF/B-VIII.0/β5 evaluated data at 14.5 MeV. The new normalization factor obtained by the GMA code was 1.0163 with respect to originally reported values. Only two data points, at the lowest incident-neutron energies, were slightly moved in energy to avoid interpolation artifacts.

It can be seen from Figs. 8 and 11 that the GMA evaluated results for the $^{238}\text{U}(n,f)/^{235}\text{U}(n,f)$ ratio change only within GMA reported uncertainties for the entire energy range shown. In addition to that, changes are small above 0.8 MeV. fissionTPC $^{238}\text{U}(n,f)/^{235}\text{U}(n,f)$ ratio data agree with the evaluated results within the reported uncertainties above 1.5 MeV. However, below 1.5 MeV, the fissionTPC experimental differ systematically from the evaluated results. The $^{238}\text{U}(n,f)$ cross section is a threshold reaction and it is small below 1.5 MeV. It is an experimental challenge to get the cross

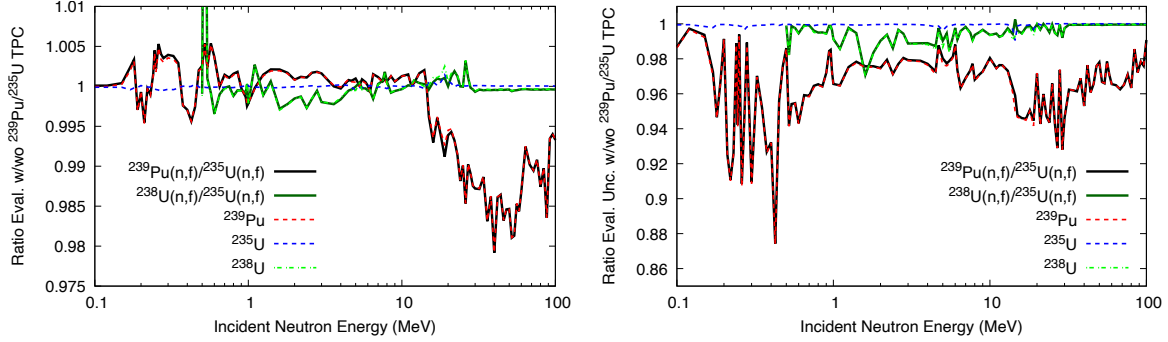


Figure 8: The impact of including fissionTPC data on evaluated $^{235,238}\text{U(n,f)}$ and $^{239}\text{Pu(n,f)}$ cross sections (left-hand side) and uncertainties (right-hand side) is shown.

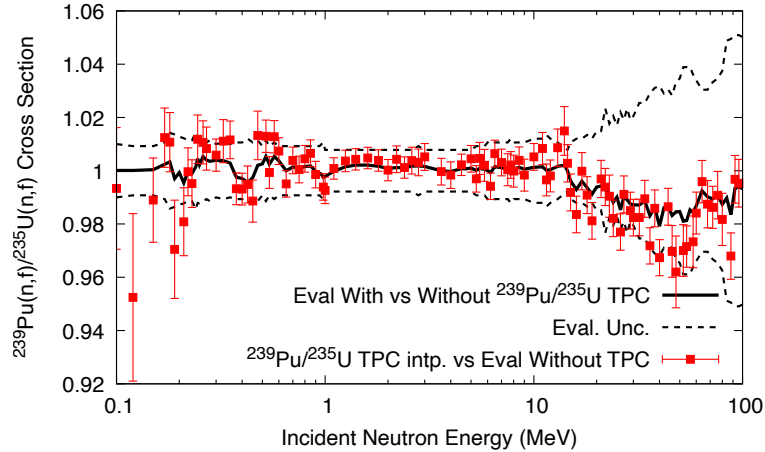


Figure 9: The impact of including fissionTPC data on evaluated $^{239}\text{Pu(n,f)}/^{235}\text{U(n,f)}$ cross sections is illustrated. It is also shown that fissionTPC data agree in general with evaluated results without these new data within their respective uncertainties.

section correctly there leading to potential larger bias in previous and fissionTPC data. It should be mentioned that fissionTPC data come with considerable uncertainties in the energy range in question; that is with total uncertainties from (4–102%). The major drivers of uncertainties up to 1.5 MeV are counting-statistics and impurity uncertainties. The large counting-statistics uncertainties reflect the fact that the experimentalists are trying to measure a cross section in its threshold region. The large impurity uncertainties are related to a significant ^{235}U contamination (0.5%). Below 1.5 MeV, the ^{235}U cross section is up to three orders of magnitude larger than the ^{238}U cross section (Fig. 10); a ^{235}U contamination of 0.5% can lead to a significant correction and large uncertainties. Hence, discrepancies between fissionTPC $^{238}\text{U(n,f)}/^{235}\text{U(n,f)}$ ratios and the NDS values below 1.5 MeV could possibly be caused by issues in the former data. Thus, it is realistic that the evaluated ratio does not significantly change below 1.5 MeV (that is outside evaluated uncertainties) to correspond to fissionTPC data that are rather uncertain in that energy range.

The impact of fissionTPC data on the evaluated uncertainties is only modest for all energies as can be observed from Fig. 8. That can be in part attributed to larger total uncertainties of the fissionTPC $^{238}\text{U(n,f)}/^{235}\text{U(n,f)}$ ratios compared to those reported for $^{239}\text{Pu(n,f)}/^{235}\text{U(n,f)}$; the lowest uncertainties for the former are 0.6% while they are 0.4% for the latter (on the GMA grid), and average uncertainties above 1.0% are reported for the former while they are below 1.0% for the latter. In addition to that, it

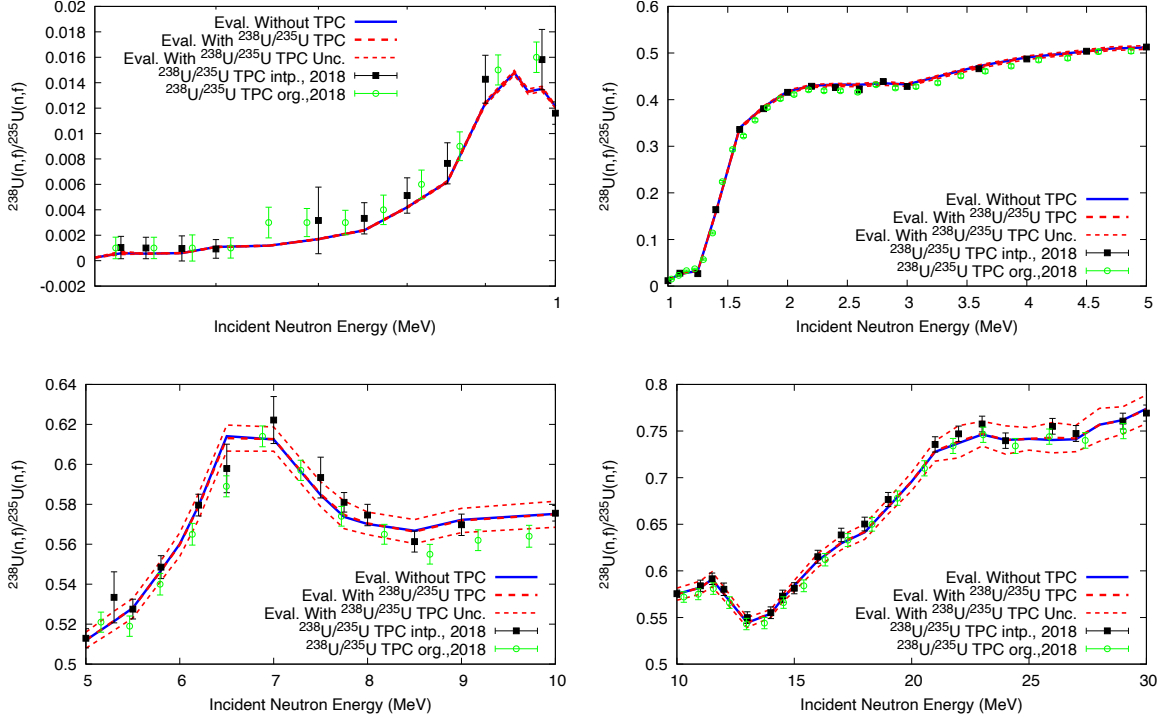


Figure 10: Evaluated $^{238}\text{U}(n,\text{f})/^{235}\text{U}(n,\text{f})$ cross sections are shown including (red thick dashed line) and excluding (blue solid line) fissionTPC data. Evaluated uncertainties including fissionTPC data are also shown in less thick red dashed lines. fissionTPC data as reported by the collaboration are shown in green, while the interpolated and renormalized data are shown in black.

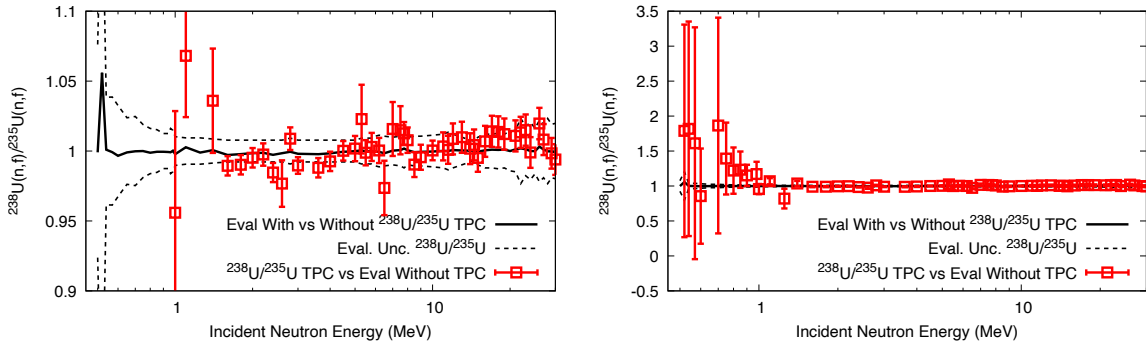


Figure 11: The impact of including fissionTPC data on evaluated $^{238}\text{U}(n,\text{f})/^{235}\text{U}$ cross sections is illustrated. It is also shown that fissionTPC data agree in general with evaluated results above 1.5 MeV without these new data within their respective uncertainties.

is discussed in Subsection 3.5 that the experimental covariances for $^{238}\text{U}(n,\text{f})$ cross sections in the GMA database might need to be revised for missing uncertainties via templates of expected measurement uncertainties.

3.2 Should Tovesson *et al.* Data Above 13 MeV be Included into the NDS Database?

As mentioned in Section 3.1.1, $^{239}\text{Pu}(\text{n},\text{f})$ cross section data at high incident-neutron energies (above 10 MeV) assume up to 2% lower values if fissionTPC data are implemented. This has important implications for past data sets. As documented in Ref. [6], the data of Tovesson *et al.* [10] and Shcherbakov *et al.* [16] led to questions that could not be satisfactorily solved before the release of the 2018 NDS version. These two data sets, as shown in Fig. 12, span between them the space of possible experimental values above 14 MeV. Other data, *e.g.*, of Staples *et al.* [17] and Lisowski *et al.* [18], go through the middle of Tovesson and Shcherbakov data. The NDS committee was unsure which one of those two data sets—Tovesson *et al.* and Shcherbakov *et al.*—was more reliable, and finally decided to cut Tovesson *et al.* data above 13 MeV from the evaluation.

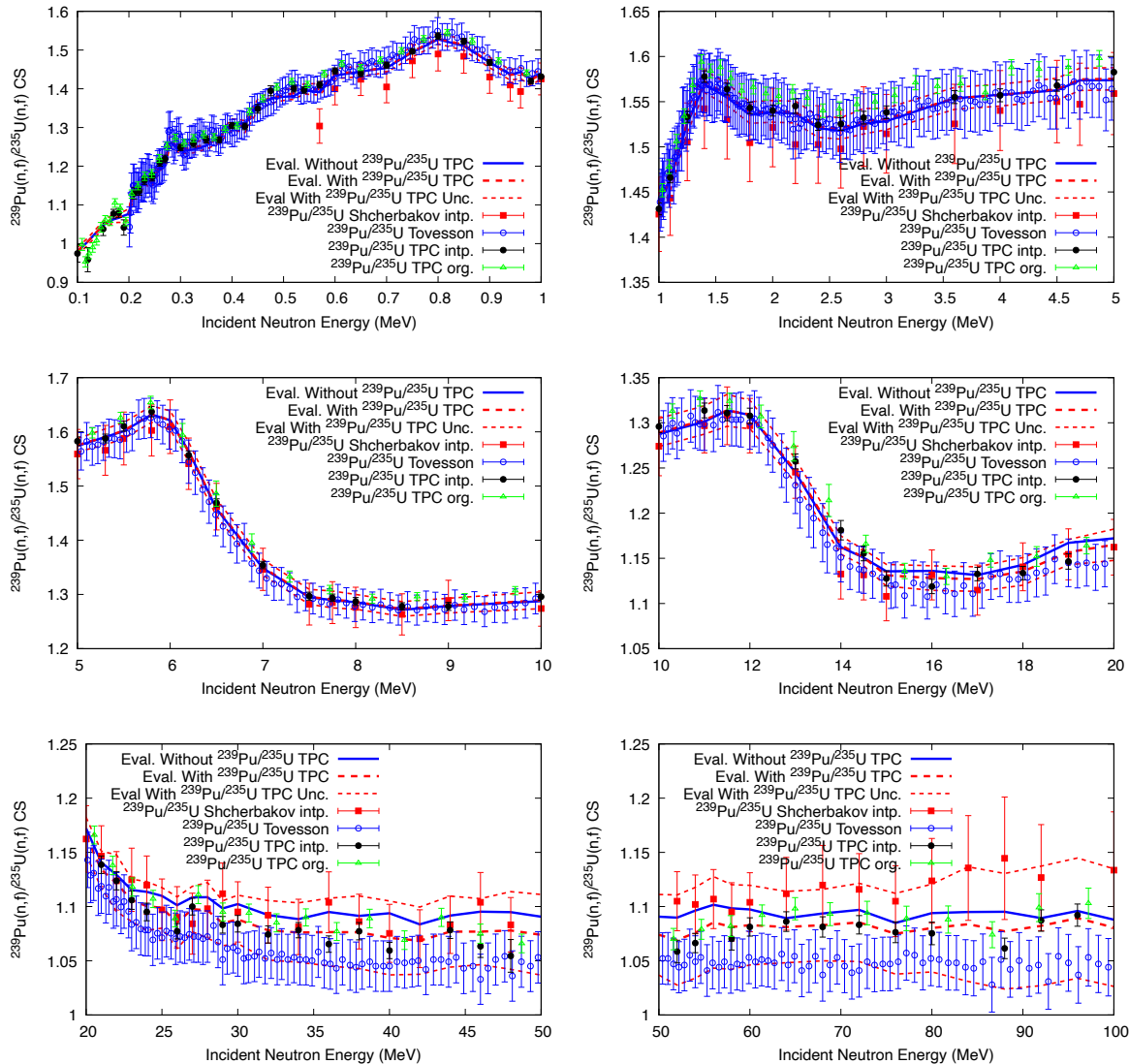


Figure 12: The same as for Fig. 7 including a comparison to Tovesson (in blue) and Shcherbakov (in red) data.

However, recent fissionTPC $^{239}\text{Pu}(\text{n},\text{f})/^{235}\text{U}(\text{n},\text{f})$ cross sections also point to lower values than Shcherbakov *et al.* Hence, DN would recommend to reassess whether Tovesson *et al.* should be included after all above 13 MeV as they seem to represent indeed a physically possible data set. This

is especially true as the fissionTPC collaboration meticulously studied all possible physics effects that could affect the fission cross section.

3.3 Should USU be Re-formulated to Account for Partially Independent Measurements?

The uncertainties compared in Fig. 8 only show the impact of fissionTPC data on GMA evaluated uncertainties. However, these GMA uncertainties are NOT the total uncertainties reported by the NDS community for the 2018 NDS version. For the 2018 NDS release, a fully-correlated USU uncertainty of 1.2% was added for all three fission observables for fast energies [6]. If the same procedure is undertaken for this evaluation, all reductions of uncertainties gained through fissionTPC data would be completely drowned out by the much larger USU uncertainty.

However, DN would strongly question whether that is justified. One can argue that there is a significant spread in previous data, and evaluated uncertainties should reflect that. This is especially true because most of the underlying experimental data were measured with one and the same technology—fission and ionization chambers. There is no way to exclude any potential systematic effect of this technique and uncertainties should account for that [11]. However, this comes with a caveat: This is only true if there is no “validation measurement” that verifies the trend of data obtained from the same technique with a completely different technology. DN would argue that some parts of the fissionTPC measurement (namely the detector efficiency) employ a different technology—a time-projection chamber instead of a fission or ionization chamber.

Hence, fissionTPC data verified the evaluated mean-value trend obtained by averaging over data from several hundreds of fission-chamber measurements, and, thus, gives us more confidence in these past data. DN would recommend that the NDS committee might want to consider revisiting the USU formulation to take into account validation from a partially independent measurement.

3.4 Should the Procedure for Assessing Outlying Uncertainties be Adapted?

Another issue that arises when including new data is the one of assessing outlying uncertainties. Some data points are simply outlying because of statistics or systematic effects. This is a well-known fact and, thus, outlying uncertainties are justified for individual points that are outlying out of an otherwise agreeing trend.

However, the question arises if that should be done for a group of systematically outlying data in the same way that we are currently assessing outlying uncertainties for NDS evaluations. Right now, outlying uncertainties for individual points and larger trends are quantified with respect to the evaluated curve before including the data. However, by this step-wise procedure—namely, quantifying outlying uncertainties of new data with respect to the bulk of existing data—one implicitly favors the trend obtained by already existing data and penalizes new data, effectively skewing evaluated results to past data.

One might want to consider doing an evaluation without outlying uncertainties for all data, getting a mean trend and then quantifying outlying uncertainties for all data at once. That would lead to a more unbiased procedure for all data at once and would allow newer data sets to guide the evaluation with the same weight as past data.

3.5 Future Work Needed on NDS Database

It was discussed in Section 3.1.1 and shown in Fig. 8 that most of the changes of the fissionTPC data apply to ^{238}U and ^{239}Pu data, while ^{235}U remains largely unchanged. Also, larger changes are observed for ^{239}Pu than for ^{238}U cross sections. One part of the reason behind this is that ^{235}U data are distinctly more abundant compared to ^{239}Pu data due to the many ratio measurements in the database. However, this does not explain the lower impact on $^{238}\text{U}(\text{n},\text{f})$ cross sections.

Part of the reason for that could be unrealistically low uncertainties reported for some past experimental $^{235,238}\text{U}(\text{n},\text{f})$ cross sections in the database. While a template of expected measurement uncertainties was applied to all experimental $^{239}\text{Pu}(\text{n},\text{f})$ covariances in Ref. [13], this was not undertaken for $^{235,238}\text{U}(\text{n},\text{f})$ experiments in the GMA database. This additional analysis should be undertaken as well for more comprehensive and reliable GMA evaluated mean values and uncertainties.

4 Counter-checking Results Obtained Above

Vladimir Pronyaev used the information above on $^{238}\text{U}(\text{n},\text{f})/^{235}\text{U}(\text{n},\text{f})$ ratios to re-run the evaluation and counter-check for possible mistakes. He used a previous version of $^{239}\text{Pu}(\text{n},\text{f})/^{235}\text{U}(\text{n},\text{f})$ fissionTPC data (as documented in LA-UR-21-24093 version 1). Despite some differences in data, we see whether the input deck works and whether the general trends observed above hold. Below this check is summarized.

4.1 $^{239}\text{Pu}(\text{n},\text{f})/^{235}\text{U}(\text{n},\text{f})$ Cross Sections

The GMA fit was undertaken by Vladimir Pronyaev with the total GMA database and few latest data sets including new n_TOF data for $^{238}\text{U}(\text{n},\text{f})/^{235}\text{U}(\text{n},\text{f})$ ratio and $^{239}\text{Pu}(\text{n},\text{f})/^{235}\text{U}(\text{n},\text{f})$ and $^{238}\text{U}(\text{n},\text{f})/^{235}\text{U}(\text{n},\text{f})$ fissionTPC data. Denise Neudecker and Vladimir Pronyaev use the same code. The reader should note that the GMA database used by V. Pronyaev is different from the one used by D. Neudecker. As mentioned above, the $^{239}\text{Pu}(\text{n},\text{f})/^{235}\text{U}(\text{n},\text{f})$ fissionTPC data used by V. Pronyaev are the ones as documented in LA-UR-21-24093 version 1. They differ from the data above by small fluctuations (choice of the random-number generator, and small fix in attenuation correction) as well as a slightly decreased normalization (from 2% higher than ENDF/B-VIII.0 previously to now being 1.2% too high). The normalization does not matter at all for the fit as the data are treated as “shape”. The small fluctuations in shape should be minimal.

New $^{239}\text{Pu}(\text{n},\text{f})/^{235}\text{U}(\text{n},\text{f})$ fissionTPC data are very consistent (in the limits of the experimental uncertainties which are low) with the GMA fit excluding fissionTPC data until 20 MeV. Contrary to that, the data are low in the energy range between 20 and 90 MeV (see Fig. 13). Including fissionTPC data in the GMA fit influences the evaluation in this energy range significantly as already observed above. This is shown in more detail in Fig. 13.

Tovesson *et al.* data [10] are consistent with fissionTPC data up to 2 MeV, and are slightly lower from 14–20 MeV. They are inconsistent with fissionTPC data and the GMA fit including fissionTPC data above 20 MeV as shown in Fig. 14.

The reason behind the higher values of the GMA fit are clear from Fig. 37.c of Ref. [6] and Fig. 14, where additionally absolute ratio data by Shcherbakov *et al.* [16], Staples *et al.* [17] and by Lisowski *et al.* [18] are shown. There are many other absolute and shape data for $^{239}\text{Pu}(\text{n},\text{f})$ and $^{238}\text{Pu}(\text{n},\text{f})/^{235}\text{U}(\text{n},\text{f})$ below 20 MeV which fixed the absolute $^{239}\text{Pu}(\text{n},\text{f})$ cross section in the whole energy range. As we see, including fissionTPC data in the GMA fit decreases the evaluated cross section by maximally 1.5% between 20 and 90 MeV. These new data resolve existing discrepancies between data by Lisowski *et al.* from one side and Shcherbakov *et al.* and Staples *et al.* from other side. The new fit agrees very well with Lisowski *et al.* data.

All these fits are preliminary; the reason for that is that one needs to reassess (increase) outlying uncertainties for past data (like Shcherbakov’s and Staples’) based on the new evaluated curve. That will lead to a slightly decreased weight of the previous data, and, hence a further decrease of the evaluated mean values from 20–90 MeV. We see also that Tovesson’s data—mostly consistent with the previous standard evaluation below 14 MeV—have rather different shape in the whole energy range. The standards committee could indeed discuss the existing discrepancies and inclusion of Tovesson’s data above 14 MeV in the fit (see Fig. 15). Vladimir Pronyaev encourages LANL/ fissionTPC experimentalists to discuss this and provide an answer to the standard committee what physics cause may

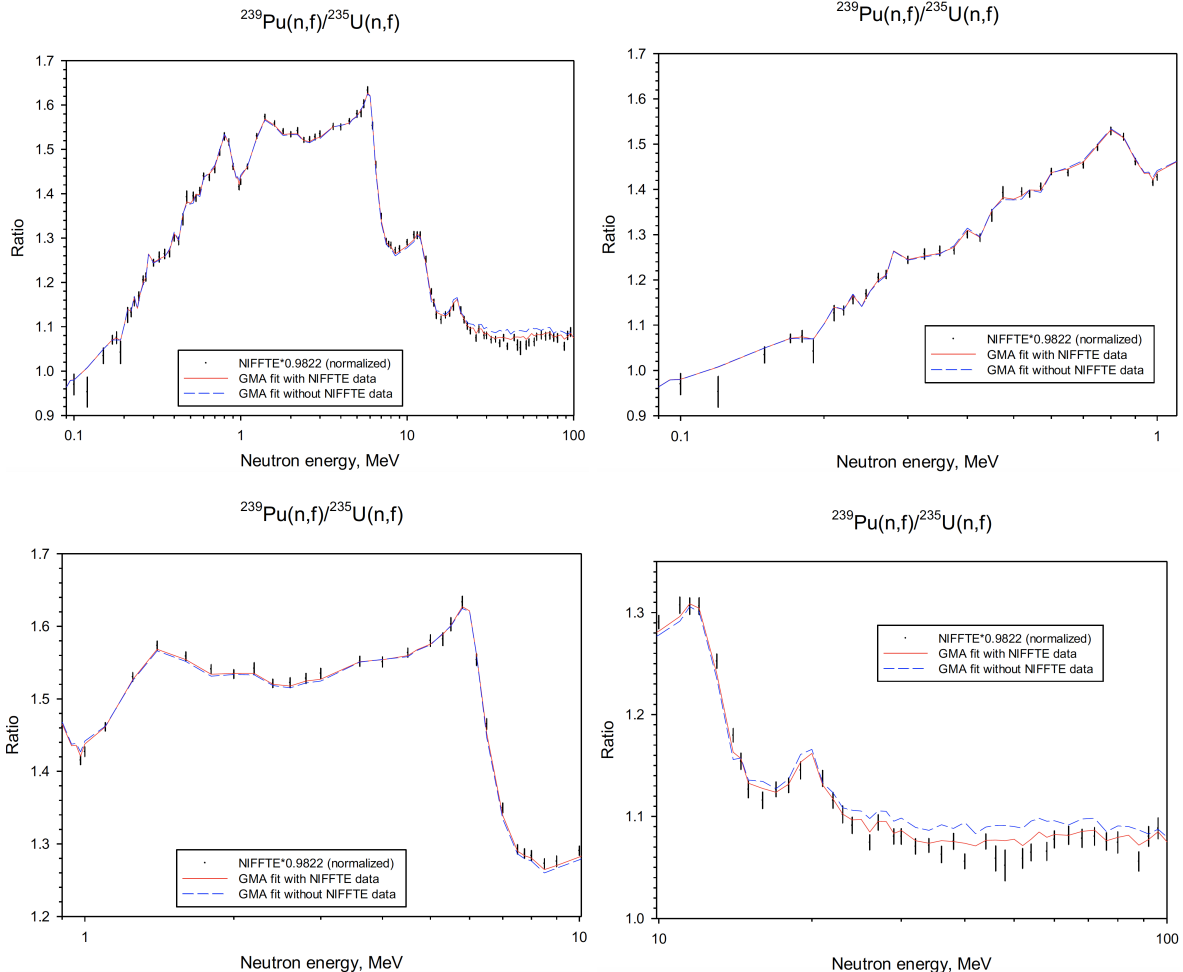


Figure 13: Evaluated $^{239}\text{Pu}(\text{n},\text{f})/^{235}\text{U}(\text{n},\text{f})$ cross sections are shown including (red solid line) and excluding (blue dashed line) fissionTPC data. Normalized fissionTPC data are shown in black.

lead to the different shapes between fissionTPC, Lisowski, Staples and Tovesson data, when uncertainty in the flux are excluded in the ratio but detectors are different.

As shown in Fig. 15, the shape of fissionTPC data is consistent with the shape of the GMA fit in the limits of 2% in the energy range covering two and half decades. The difference in the local area 30–60 MeV can be also seen.

4.2 $^{238}\text{U}(\text{n},\text{f})/^{235}\text{U}(\text{n},\text{f})$ Cross Sections

Data for $^{238}\text{U}(\text{n},\text{f})/^{235}\text{U}(\text{n},\text{f})$ ratios are obtained in a narrower energy range; they are consistent with the GMA fit above 1.5 MeV, which includes fissionTPC data and the whole GMA database (Fig. 16) as described in this section. The shape ratio in Fig. 16 shows a small offset of about 2% between 1.5 MeV and 30 MeV.

4.3 General Remarks

- GMA has an option to include variances and a total correlation matrix in the DATA.GMA file. This was employed for absolute cross sections evaluated with R-matrix theory. This option could be used for fissionTPC data. Then, the total fissionTPC covariance matrix can be directly included in the fit without approximations. However, to this end the data need to be transformed

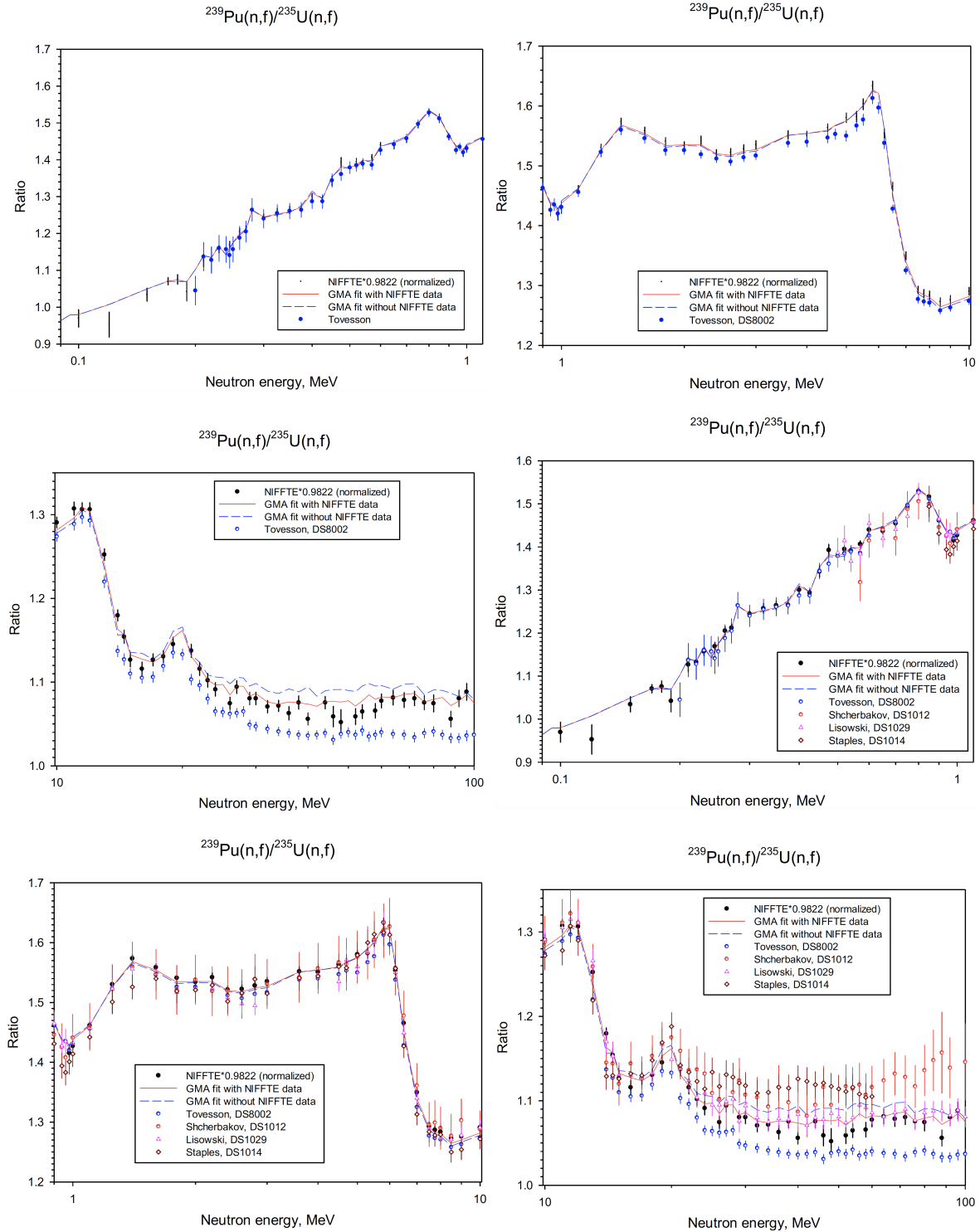


Figure 14: Evaluated $^{239}\text{Pu}(\text{n},\text{f})/^{235}\text{U}(\text{n},\text{f})$ cross sections are shown including (red solid line) and excluding (blue dashed line) fissionTPC data. Various other data sets are shown for comparison.

to be on the GMA grid. Also, it is unclear to D. Neudecker how to include cross-correlations between different data sets.

- Discrepancies between Tovesson's and Lisowski's data above 14 MeV should be discussed.

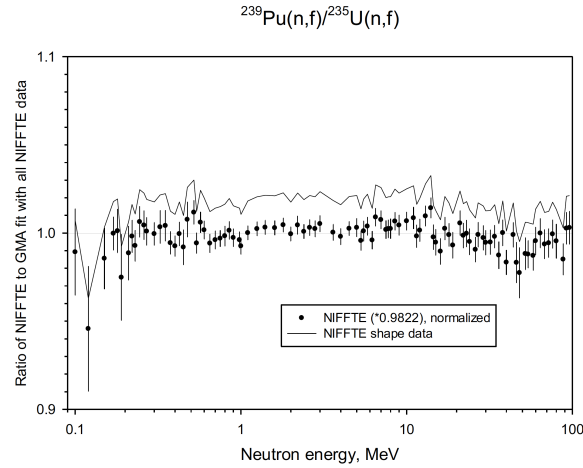


Figure 15: The impact of including fissionTPC data on evaluated $^{239}\text{Pu}(\text{n},\text{f})/^{235}\text{U}(\text{n},\text{f})$ cross sections is illustrated. It is also shown that fissionTPC data agree in general with evaluated results.

- It is strange for V. Pronyaev that the fissionTPC shape data have very low cross-energy correlations. A discussion with experimentalists might be needed at the next standard meeting.
- The general trends seen by D. Neudecker and V. Pronyaev when including the two data sets are very similar. Hence, any major issues in the inclusion can be excluded and the input deck seem fine.

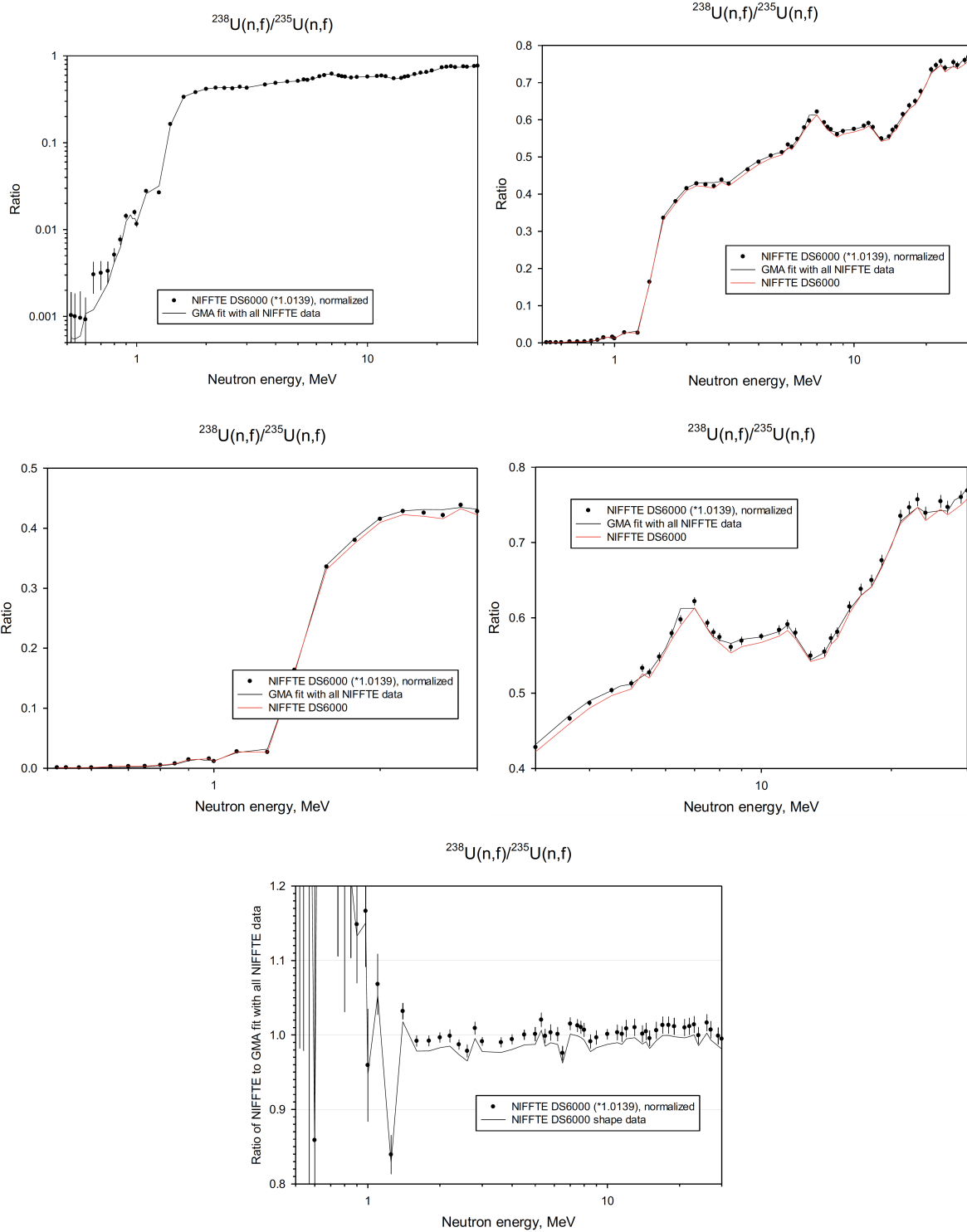


Figure 16: Evaluated $^{238}\text{U}(n,f)/^{235}\text{U}(n,f)$ cross sections are shown including (black line) fissionTPC data (black dots).

5 Summary and Conclusions

In this report it is shown how $^{238}\text{U}(n,f)/^{235}\text{U}(n,f)$ and $^{239}\text{Pu}(n,f)/^{235}\text{U}(n,f)$ fissionTPC data were included in the current NDS (Neutron Data Standards) database in answer to NDS needs but also to an

NCSP FY21 milestone of DN. The data sets were included independently by two people, D. Neudecker and V. Pronyaev, to counter-check results and make sure that no major issues were overlooked when including the data. The general trends found by both analyses agreed well with each other. The hope is that this report provides sufficient information for the NDS committee to be able to reach a decision whether these new data by the fissionTPC collaboration should be officially included in the NDS database or not.

The evaluated results of $^{238}\text{U}(\text{n},\text{f})/^{235}\text{U}(\text{n},\text{f})$ cross sections change only little because of larger fissionTPC uncertainties for this ratio and a missing analysis on whether past data of this observable in the GMA database reported all pertinent uncertainties.

The evaluated results of $^{239}\text{Pu}(\text{n},\text{f})/^{235}\text{U}(\text{n},\text{f})$ cross sections change little below 10 MeV. One should consider that the new $^{239}\text{Pu}(\text{n},\text{f})/^{235}\text{U}(\text{n},\text{f})$ fissionTPC data set reports one of the lowest uncertainties of all of the $^{239}\text{Pu}(\text{n},\text{f})$ measurements in the GMA database underlying NDS evaluations. In addition to that, experimental $^{239}\text{Pu}(\text{n},\text{f})$ covariances in the GMA database were revisited for missing known uncertainties of experimental data in Ref. [13]. Hence, the small change in evaluated results below 10 MeV points to that previous data using mainly fission and ionization chambers give on average the same trend as data measured by the fissionTPC. This is very interesting indeed as it shows that fissionTPC data validate on average data taken previously with fission and ionization chambers, and thus verifies NDS data of the last decades.

However, evaluated results of $^{239}\text{Pu}(\text{n},\text{f})/^{235}\text{U}(\text{n},\text{f})$ cross sections including fissionTPC data differ by up to 2% above 10 MeV from those excluding the new experimental data; fissionTPC data point to increasingly lower values above 10 MeV. This indicates that data previously rejected as too low above 13 MeV by Tovesson *et al.* could be after all representing physics adequately. It should be discussed again by the NDS committee whether Tovesson data could be included after all.

In addition to that fissionTPC data raised the following issues for the NDS committee to discuss:

- Should quantifying USU (unknown sources of uncertainties) uncertainties be re-formulated to consider the impact independent “validation measurements” have on these uncertainties?
- Should outlying uncertainties be applied to the database as a whole once it is frozen for an NDS version rather than quantifying outlying uncertainties always with respect to the already existing database?
- It is clear that all experimental covariances in the NDS database should be re-visited with templates of expected measurement uncertainties to exclude that GMA evaluated uncertainties are underestimated because of missing but known uncertainties. It might be good to discuss where the biggest needs are and then concentrate on those. An e-mail discussion led to the conclusion that we first focus on $^{235}\text{U}(\text{n},\text{f})$ and subsequently on $^{238}\text{U}(\text{n},\text{f})$ cross sections.

Acknowledgments

Work at LANL was carried out under the auspices of the National Nuclear Security Administration (NNSA) of the U.S. Department of Energy (DOE) under contract 89233218CNA000001. DN gratefully acknowledges partial support of the Advanced Simulation and Computing program at LANL and the DOE Nuclear Criticality Safety Program, funded and managed by NNSA for the DOE.

References

- [1] N.S. Bowden et al., “Directional fast neutron detection using a time projection chamber,” *NUCL. INSTRUM. METHODS PHYS. RES. SECT A* **624**, 153 (2010).
- [2] M. Heffner et al., “A time projection chamber for high accuracy and precision fission cross-section measurements,” *NUCL. INSTRUM. METHODS PHYS. RES. SECT A* **759**, 50 (2014).
- [3] L. Snyder et al., “Performance of a MICROMEGAS-based TPC in a high-energy neutron beam,” *NUCL. INSTRUM. METHODS PHYS. RES. SECT A* **881**, 1 (2018).
- [4] R.J. Casperson et al., “Measurement of the normalized $^{238}\text{U}(\text{n,f})/^{235}\text{U}(\text{n,f})$ cross section ratio from threshold to 30 MeV with the NIFFTE fission Time Projection Chamber,” *PHYS. REV. C* **97**, 034618 (2018).
- [5] L. Snyder *et al.*, “Measurement of the $^{239}\text{Pu}(\text{n,f})/^{235}\text{U}(\text{n,f})$ Cross Section Ratio with the NIFFTE fissionTPC,” TO BE SUBMITTED TO *NUCL. DATA SHEETS*, **xx**, **xx-xx** (2021); Lawrence Livermore National Laboratory Report LLNL-TR-788566 (2020).
- [6] A.D. Carlson et al., “Evaluation of the Neutron Data Standards,” *NUCL. DATA SHEETS* **148**, 143 (2018).
- [7] M.B. Chadwick et al., “ENDF/B-VII.1 Nuclear Data for Science and Technology: Cross Sections, Covariances, Fission Product Yields and Decay Data,” *NUCL. DATA SHEETS* **112**, 2887 (2011).
- [8] D.A. Brown et al., “ENDF/B-VIII.0: The 8th Major Release of the Nuclear Reaction Data Library with CIELO-project Cross Sections, New Standards and Thermal Scattering Data,” *NUCL. DATA SHEETS* **148**, 1–142 (2018).
- [9] W.P. Poenitz and S.E. Aumeier, “The Simultaneous Evaluation of the Standards and Other Cross Sections of Importance for Technology,” Argonne National Laboratory Report ANL/NDM-139 (1997).
- [10] F. Tovesson et al., “Cross Sections for $^{239}\text{Pu}(\text{n,f})$ and $^{241}\text{Pu}(\text{n,f})$ in the Range $E_n = 0.01$ eV to 200 MeV,” *NUCLEAR SCIENCE AND ENGINEERING* **165**, 224–231 (2010).
- [11] R. Capote et al., “Unrecognized Sources of Uncertainties (USU) in Experimental Nuclear Data,” *NUCL. DATA SHEETS* **163**, 191–227 (2020).
- [12] A.D. Carlson et al., “International Evaluation of Neutron Cross Section Standards,” *NUCL. DATA SHEETS* **110**, 32150–3324 (2009).
- [13] D. Neudecker et al., “Applying a Template of Expected Uncertainties to Updating $^{239}\text{Pu}(\text{n,f})$ Cross-section Covariances in the Neutron Data Standards Database,” *NUCL. DATA SHEETS*, 228–248 (2020).
- [14] D. Neudecker, “ARIADNE—A Program Estimating Covariances in Detail for Neutron Experiments,” *EUROP. PHYS. J. N* **4**, 34 (2018).
- [15] D. Neudecker et al., “Information Files of $^{238}\text{U}(\text{n,f})/^{235}\text{U}(\text{n,f})$ NIFFTE fissionTPC Cross-sections for the Neutron Data Standards Project,” Los Alamos National Laboratory Report LA-UR-18-23788 (2018).
- [16] O. Shcherbakov et al., “Neutron-induced fission of ^{233}U , ^{238}U , ^{232}Th , ^{239}Pu , ^{237}Np , ^{nat}Pb and ^{209}Bi relative to ^{235}U in the energy range 1–200 MeV,” *JOUR. OF NUCLEAR SCIENCE AND TECHNOLOGY SUPPL.* **2** **39**, 230–233 (2002).

[17] P. Staples and K. Morley, “Neutron-Induced Fission Cross-Section Ratios for ^{239}Pu , ^{240}Pu , ^{242}Pu , and ^{244}Pu Relative to ^{235}U from 0.5 to 400 MeV,” *NUCL. SCIENCE AND ENG.* **129**, 149–163 (1998).

[18] P.W. Lisowski, J.L. Ullmann, S.J. Balestrini *et al.*, “Neutron Induced Fission Cross Section Ratios for ^{232}Th , $^{235,238}\text{U}$, ^{237}Np and ^{239}Pu from 1 to 400 MeV,” Proc. of the Conf. on Nucl. Data for Science and Technol., Mito 1988, 97–99 (1988); P.W. Lisowski, A. Gavron, W.E. Parker *et al.*, “Fission Cross Sections in the Intermediate Energy Region,” Proc. of a Specialists’ Meeting on Neutron Cross Section Standards for the Energy Region above 20 MeV, Report NEANDC-305, 177–186 (1991); A.D. Carlson, O.A. Wasson, P.W. Lisowski *et al.*, “A Study of the $^{235}\text{U}(\text{n},\text{f})$ Cross Section in the 3 to 30 MeV Energy Region,” Proc. of the Conf. on Nucl. Data for Science and Technol., Mito 1988, 1029–1032 (1988).

[19] G. Potel Aguilar *et al.*, “LLNL Evaluation of $\text{n}+^{239}\text{Pu}$,” Lawrence Livermore National Laboratory Report LLNL-MI-834591 (2022).

Below the output files for the $^{235,8}\text{U}(\text{n},\text{f})$ and $^{239}\text{Pu}(\text{n},\text{f})$ cross sections (after fourth iteration) are shown.

A Output Files for $^{235}\text{U}(\text{n},\text{f})$ Cross Sections

1 RESULT U5(n,f)

E/MEV	CS/B	DCS/B	DCS/\%	DIF/\%	CS*SQRT(E)
0.2530E-07	587.31459496	1.37570079	0.2	0.00	0.09342
0.9400E-05	247.30059193	1.06185337	0.4	0.00	0.75821
0.1500E-03	21.22286171	0.08951197	0.4	0.00	0.25993
0.2500E-03	20.76112503	0.09193331	0.4	0.00	0.32826
0.3500E-03	13.16286402	0.06236034	0.5	-0.00	0.24625
0.4500E-03	13.79971482	0.06611413	0.5	0.00	0.29274
0.5500E-03	15.21492095	0.07566564	0.5	0.00	0.35682
0.6500E-03	11.53710164	0.05760908	0.5	-0.00	0.29414
0.7500E-03	11.12075297	0.05603339	0.5	0.00	0.30455
0.8500E-03	8.23391249	0.04193499	0.5	0.00	0.24006
0.9500E-03	7.52192108	0.03857013	0.5	0.00	0.23184
0.1500E-02	7.32375874	0.03491422	0.5	0.00	0.28365
0.2500E-02	5.39437533	0.02979168	0.6	0.00	0.26972
0.3500E-02	4.80036881	0.02626282	0.5	0.00	0.28399
0.4500E-02	4.27853357	0.02279604	0.5	0.00	0.28701
0.5500E-02	3.84538971	0.02110836	0.5	0.00	0.28518
0.6500E-02	3.30276371	0.01888952	0.6	0.00	0.26628
0.7500E-02	3.24773665	0.01722690	0.5	0.00	0.28126
0.8500E-02	3.00822300	0.01647460	0.5	0.00	0.27734
0.9500E-02	3.11456681	0.01663127	0.5	0.00	0.30357
0.1500E-01	2.49921150	0.01205092	0.5	0.00	0.30609
0.2000E-01	2.35110066	0.02949412	1.3	0.00	0.33250
0.2400E-01	2.16301685	0.01065758	0.5	0.00	0.33509
0.3000E-01	2.07611152	0.01201176	0.6	-0.00	0.35959
0.4500E-01	1.85093311	0.00997416	0.5	-0.00	0.39264
0.5500E-01	1.81302851	0.00998202	0.6	0.00	0.42519

0.6500E-01	1.75373453	0.00951002	0.5	0.00	0.44712
0.7500E-01	1.68089233	0.00895997	0.5	-0.00	0.46033
0.8500E-01	1.59565843	0.00899134	0.6	0.00	0.46521
0.9500E-01	1.57609124	0.00900539	0.6	0.00	0.48578
0.1000E+00	1.58590960	0.00974844	0.6	0.00	0.50151
0.1200E+00	1.49922543	0.00882494	0.6	0.00	0.51935
0.1500E+00	1.43244568	0.00855555	0.6	0.00	0.55478
0.1700E+00	1.39995130	0.00913922	0.7	0.00	0.57721
0.1800E+00	1.39535105	0.01261375	0.9	0.00	0.59200
0.1900E+00	1.36868995	0.01078656	0.8	-0.00	0.59660
0.2000E+00	1.34916016	0.01045572	0.8	0.00	0.60336
0.2100E+00	1.34895110	0.00990468	0.7	0.00	0.61817
0.2200E+00	1.32305482	0.00928594	0.7	-0.00	0.62057
0.2300E+00	1.29771435	0.00903581	0.7	-0.00	0.62236
0.2350E+00	1.30246658	0.00970176	0.7	-0.00	0.63139
0.2400E+00	1.29183185	0.01047658	0.8	-0.00	0.63287
0.2450E+00	1.29172616	0.00970946	0.8	-0.00	0.63937
0.2500E+00	1.28068709	0.00853228	0.7	-0.00	0.64034
0.2600E+00	1.26303792	0.00914654	0.7	-0.00	0.64403
0.2700E+00	1.24823830	0.00831209	0.7	-0.00	0.64860
0.2800E+00	1.23321938	0.00805829	0.7	0.00	0.65256
0.3000E+00	1.22951886	0.00740817	0.6	-0.00	0.67344
0.3250E+00	1.23483440	0.00870698	0.7	-0.00	0.70396
0.3500E+00	1.21473978	0.00740991	0.6	-0.00	0.71865
0.3750E+00	1.21745836	0.00832283	0.7	-0.00	0.74554
0.4000E+00	1.18438855	0.00800335	0.7	0.00	0.74907
0.4250E+00	1.20097742	0.00929511	0.8	0.00	0.78294
0.4500E+00	1.16358876	0.00812777	0.7	0.00	0.78056
0.4750E+00	1.13868972	0.00821498	0.7	0.00	0.78479
0.5000E+00	1.14033119	0.00685356	0.6	0.00	0.80634
0.5200E+00	1.13871582	0.00836553	0.7	0.00	0.82114
0.5400E+00	1.12133543	0.00704752	0.6	0.00	0.82401
0.5700E+00	1.13804446	0.00803474	0.7	-0.00	0.85920
0.6000E+00	1.10867727	0.00673130	0.6	-0.00	0.85878
0.6500E+00	1.11889254	0.00621611	0.6	-0.00	0.90208
0.7000E+00	1.11563721	0.00638000	0.6	-0.00	0.93341
0.7500E+00	1.13116739	0.00627024	0.6	-0.00	0.97962
0.8000E+00	1.10977282	0.00613058	0.6	-0.00	0.99261
0.8500E+00	1.11873844	0.00643096	0.6	-0.00	1.03143
0.9000E+00	1.14317366	0.00642132	0.6	-0.00	1.08451
0.9400E+00	1.17190591	0.00692860	0.6	-0.00	1.13620
0.9600E+00	1.19809887	0.00772057	0.6	-0.00	1.17389
0.9800E+00	1.20567571	0.00865468	0.7	-0.00	1.19356
0.1000E+01	1.20158838	0.00615534	0.5	-0.00	1.20159
0.1100E+01	1.19271046	0.00579843	0.5	-0.00	1.25093
0.1250E+01	1.20928116	0.00582382	0.5	-0.00	1.35202
0.1400E+01	1.22626261	0.00615928	0.5	-0.00	1.45093
0.1600E+01	1.25222507	0.00600493	0.5	-0.00	1.58395
0.1800E+01	1.27007834	0.00634965	0.5	-0.00	1.70399
0.2000E+01	1.28602864	0.00667341	0.5	-0.00	1.81872

0.2200E+01	1.27659133	0.00663120	0.5	-0.00	1.89349
0.2400E+01	1.26299448	0.00648229	0.5	-0.00	1.95662
0.2600E+01	1.25483626	0.00682643	0.5	-0.00	2.02336
0.2800E+01	1.23699122	0.00757873	0.6	-0.00	2.06988
0.3000E+01	1.21469282	0.00635671	0.5	-0.00	2.10391
0.3600E+01	1.16346985	0.00584127	0.5	-0.00	2.20753
0.4000E+01	1.13480224	0.00582705	0.5	-0.00	2.26960
0.4500E+01	1.11460939	0.00590121	0.5	-0.00	2.36444
0.4700E+01	1.09820988	0.00600487	0.5	-0.00	2.38086
0.5000E+01	1.07043289	0.00553579	0.5	-0.00	2.39356
0.5300E+01	1.05494141	0.00621688	0.6	-0.00	2.42866
0.5500E+01	1.03566472	0.00589839	0.6	-0.00	2.42885
0.5800E+01	1.03671373	0.00656037	0.6	-0.00	2.49674
0.6000E+01	1.09073116	0.00728975	0.7	-0.00	2.67173
0.6200E+01	1.17919023	0.00890442	0.8	-0.00	2.93616
0.6500E+01	1.33196652	0.00908944	0.7	-0.00	3.39586
0.7000E+01	1.54263359	0.01039373	0.7	-0.00	4.08142
0.7500E+01	1.70186172	0.01204347	0.7	-0.00	4.66074
0.7750E+01	1.73771669	0.01426102	0.8	-0.00	4.83760
0.8000E+01	1.78504642	0.01214970	0.7	-0.00	5.04887
0.8500E+01	1.79292667	0.01251555	0.7	-0.00	5.22723
0.9000E+01	1.77882624	0.01235273	0.7	-0.00	5.33648
0.1000E+02	1.75871426	0.01385549	0.8	-0.00	5.56154
0.1100E+02	1.73636738	0.01383523	0.8	-0.00	5.75888
0.1150E+02	1.70288970	0.01518990	0.9	-0.00	5.77478
0.1200E+02	1.72036788	0.01434587	0.8	-0.00	5.95953
0.1300E+02	1.88470727	0.01256882	0.7	-0.00	6.79541
0.1400E+02	2.07519127	0.01063576	0.5	-0.00	7.76465
0.1450E+02	2.07877535	0.01050051	0.5	-0.00	7.91574
0.1500E+02	2.12123257	0.01381761	0.7	-0.00	8.21550
0.1600E+02	2.15137679	0.01703387	0.8	-0.00	8.60551
0.1700E+02	2.09403856	0.01765718	0.8	-0.00	8.63394
0.1800E+02	2.05783855	0.01778306	0.9	-0.00	8.73067
0.1900E+02	2.03425464	0.01548450	0.8	-0.00	8.86711
0.2000E+02	2.02315175	0.01976628	1.0	-0.00	9.04781
0.2100E+02	2.08858475	0.02086012	1.0	-0.00	9.57110
0.2200E+02	2.11400195	0.03488060	1.6	0.00	9.91555
0.2300E+02	2.14260196	0.02646467	1.2	-0.00	10.27556
0.2400E+02	2.08703080	0.02941996	1.4	-0.00	10.22432
0.2500E+02	2.12451821	0.02421311	1.1	-0.00	10.62259
0.2600E+02	2.12568332	0.03208423	1.5	-0.00	10.83890
0.2700E+02	2.10605292	0.02667039	1.3	-0.00	10.94337
0.2800E+02	2.13202245	0.03404314	1.6	-0.00	11.28160
0.2900E+02	2.10281979	0.02694677	1.3	0.00	11.32403
0.3000E+02	2.15265806	0.02970197	1.4	-0.00	11.79059
0.3200E+02	2.13687284	0.03774713	1.8	-0.00	12.08798
0.3400E+02	2.11608032	0.03758806	1.8	-0.00	12.33876
0.3600E+02	2.03234510	0.04067337	2.0	-0.00	12.19407
0.3800E+02	1.97666860	0.04279747	2.2	-0.00	12.18500
0.4000E+02	1.99489787	0.04403440	2.2	-0.00	12.61684

0.4200E+02	1.97240534	0.03987418	2.0	-0.00	12.78265
0.4400E+02	1.96294746	0.04127649	2.1	-0.00	13.02072
0.4600E+02	1.94903657	0.03837487	2.0	-0.00	13.21901
0.4800E+02	1.91878951	0.04500855	2.3	-0.00	13.29376
0.5000E+02	1.89820829	0.04565608	2.4	-0.00	13.42236
0.5200E+02	1.90421191	0.05118178	2.7	-0.00	13.73147
0.5400E+02	1.86731042	0.05026612	2.7	-0.00	13.72187
0.5600E+02	1.88918558	0.05137728	2.7	-0.00	14.13737
0.5800E+02	1.87066248	0.04705220	2.5	-0.00	14.24654
0.6000E+02	1.84770496	0.04357028	2.4	-0.00	14.31226
0.6400E+02	1.83318985	0.03823528	2.1	-0.00	14.66552
0.6800E+02	1.76752530	0.03712905	2.1	-0.00	14.57539
0.7200E+02	1.72776957	0.03973915	2.3	-0.00	14.66061
0.7600E+02	1.73912546	0.04222827	2.4	-0.00	15.16134
0.8000E+02	1.70471865	0.04412806	2.6	-0.00	15.24747
0.8400E+02	1.69825481	0.05829968	3.4	-0.00	15.56476
0.8800E+02	1.63189059	0.05691737	3.5	-0.00	15.30849
0.9200E+02	1.59336377	0.05692054	3.6	-0.00	15.28301
0.9600E+02	1.56389467	0.05586780	3.6	-0.00	15.32298
0.1000E+03	1.58218584	0.05570713	3.5	-0.00	15.82186
0.1040E+03	1.50800500	0.05431873	3.6	-0.00	15.37869
0.1080E+03	1.56853008	0.07094293	4.5	-0.00	16.30064
0.1120E+03	1.51365298	0.06764751	4.5	-0.00	16.01900
0.1160E+03	1.53508230	0.06735412	4.4	-0.00	16.53334
0.1200E+03	1.47946837	0.06534435	4.4	-0.00	16.20676
0.1280E+03	1.47782628	0.06253309	4.2	-0.00	16.71970
0.1360E+03	1.46614775	0.06021652	4.1	-0.00	17.09807
0.1440E+03	1.44057042	0.05536641	3.8	-0.00	17.28685
0.1520E+03	1.46490806	0.06035915	4.1	-0.00	18.06060
0.1600E+03	1.44580794	0.06106477	4.2	-0.00	18.28818
0.1680E+03	1.43729504	0.06427885	4.5	-0.00	18.62947
0.1760E+03	1.45553319	0.06328414	4.3	-0.00	19.30983
0.1840E+03	1.45333002	0.06608905	4.5	-0.00	19.71393
0.1920E+03	1.44178891	0.06169190	4.3	-0.00	19.97801
0.2000E+03	1.44766510	0.06154217	4.3	-0.00	20.47308

B Output Files for $^{238}\text{U}(\text{n},\text{f})$ Cross Sections

1 RESULT U8(n,f)

E/MEV	CS/B	DCS/B	DCS/\%	DIF/\%	CS*SQRT(E)
0.5000E+00	0.00027762	0.00002120	7.6	-0.03	0.00020
0.5200E+00	0.00069438	0.00014194	20.4	0.00	0.00050
0.5400E+00	0.00061754	0.00002364	3.8	-0.00	0.00045
0.5700E+00	0.00067872	0.00002580	3.8	-0.00	0.00051
0.6000E+00	0.00119270	0.00003868	3.2	-0.00	0.00092
0.6500E+00	0.00132288	0.00003009	2.3	-0.00	0.00107
0.7000E+00	0.00189274	0.00004576	2.4	-0.00	0.00158

0.7500E+00	0.00270449	0.00004964	1.8	-0.00	0.00234
0.8000E+00	0.00465630	0.00007194	1.5	-0.00	0.00416
0.8500E+00	0.00694050	0.00009533	1.4	-0.00	0.00640
0.9000E+00	0.01416349	0.00015174	1.1	-0.00	0.01344
0.9400E+00	0.01731915	0.00019142	1.1	-0.00	0.01679
0.9600E+00	0.01592922	0.00024084	1.5	-0.00	0.01561
0.9800E+00	0.01629556	0.00020393	1.3	-0.00	0.01613
0.1000E+01	0.01455476	0.00013182	0.9	-0.00	0.01455
0.1100E+01	0.03109983	0.00025090	0.8	0.00	0.03262
0.1250E+01	0.03938532	0.00031828	0.8	0.00	0.04403
0.1400E+01	0.19403761	0.00129441	0.7	-0.00	0.22959
0.1600E+01	0.42413283	0.00254299	0.6	-0.00	0.53649
0.1800E+01	0.48697798	0.00291459	0.6	-0.00	0.65335
0.2000E+01	0.53637478	0.00321992	0.6	-0.00	0.75855
0.2200E+01	0.54792934	0.00328922	0.6	-0.00	0.81271
0.2400E+01	0.54488271	0.00328551	0.6	-0.00	0.84413
0.2600E+01	0.54116994	0.00334765	0.6	-0.00	0.87261
0.2800E+01	0.53789854	0.00370349	0.7	-0.00	0.90008
0.3000E+01	0.52462692	0.00314623	0.6	-0.00	0.90868
0.3600E+01	0.54788306	0.00321205	0.6	-0.00	1.03954
0.4000E+01	0.55598508	0.00331215	0.6	-0.00	1.11197
0.4500E+01	0.56121186	0.00347829	0.6	-0.00	1.19051
0.4700E+01	0.55922587	0.00356454	0.6	-0.00	1.21237
0.5000E+01	0.54801183	0.00326459	0.6	-0.00	1.22539
0.5300E+01	0.55037476	0.00386475	0.7	-0.00	1.26706
0.5500E+01	0.54683209	0.00369196	0.7	-0.00	1.28243
0.5800E+01	0.56681146	0.00409771	0.7	-0.00	1.36506
0.6000E+01	0.61064946	0.00471821	0.8	-0.00	1.49578
0.6200E+01	0.68269053	0.00573098	0.8	-0.00	1.69989
0.6500E+01	0.81667314	0.00617805	0.8	-0.00	2.08212
0.7000E+01	0.94508976	0.00701763	0.7	-0.00	2.50047
0.7500E+01	0.99563902	0.00793433	0.8	-0.00	2.72667
0.7750E+01	0.99874016	0.00900157	0.9	-0.00	2.78037
0.8000E+01	1.01830566	0.00760591	0.7	-0.00	2.88020
0.8500E+01	1.01534785	0.00783104	0.8	-0.00	2.96022
0.9000E+01	1.01730999	0.00770121	0.8	-0.00	3.05193
0.1000E+02	1.01129846	0.00858474	0.8	-0.00	3.19801
0.1100E+02	1.01079499	0.00884540	0.9	-0.00	3.35243
0.1150E+02	1.00641824	0.00980225	1.0	-0.00	3.41293
0.1200E+02	0.99036797	0.00912780	0.9	-0.00	3.43074
0.1300E+02	1.02653885	0.00751152	0.7	-0.00	3.70124
0.1400E+02	1.15025974	0.00689196	0.6	-0.00	4.30388
0.1450E+02	1.18603403	0.00642320	0.5	-0.00	4.51628
0.1500E+02	1.23875376	0.00877210	0.7	-0.00	4.79767
0.1600E+02	1.31496819	0.01142522	0.9	-0.00	5.25987
0.1700E+02	1.31966902	0.01200360	0.9	-0.00	5.44113
0.1800E+02	1.32107998	0.01221195	0.9	-0.00	5.60487
0.1900E+02	1.36112897	0.01173008	0.9	-0.00	5.93302
0.2000E+02	1.40787407	0.01477998	1.0	-0.00	6.29620
0.2100E+02	1.52163006	0.01625426	1.1	-0.00	6.97298

0.2200E+02	1.56113045	0.02629388	1.7	0.00	7.32235
0.2300E+02	1.60100943	0.02078643	1.3	-0.00	7.67817
0.2400E+02	1.54515977	0.02283080	1.5	-0.00	7.56971
0.2500E+02	1.57558061	0.01941506	1.2	-0.00	7.87790
0.2600E+02	1.57900043	0.02513847	1.6	-0.00	8.05135
0.2700E+02	1.56275804	0.02112250	1.4	-0.00	8.12033
0.2800E+02	1.61324193	0.02701774	1.7	-0.00	8.53647
0.2900E+02	1.60137616	0.02185299	1.4	0.00	8.62367
0.3000E+02	1.66483518	0.02376957	1.4	-0.00	9.11868
0.3200E+02	1.68222957	0.03036517	1.8	-0.00	9.51613
0.3400E+02	1.68596268	0.03080765	1.8	-0.00	9.83077
0.3600E+02	1.64966522	0.03360504	2.0	-0.00	9.89799
0.3800E+02	1.63175297	0.03615946	2.2	-0.00	10.05880
0.4000E+02	1.66035405	0.03721752	2.2	-0.00	10.50100
0.4200E+02	1.65025399	0.03428294	2.1	-0.00	10.69487
0.4400E+02	1.64106498	0.03509113	2.1	-0.00	10.88559
0.4600E+02	1.65271892	0.03328937	2.0	-0.00	11.20929
0.4800E+02	1.63457016	0.03903715	2.4	-0.00	11.32463
0.5000E+02	1.62793598	0.03997701	2.5	-0.00	11.51125
0.5200E+02	1.63179159	0.04458051	2.7	-0.00	11.76702
0.5400E+02	1.61100345	0.04394889	2.7	-0.00	11.83841
0.5600E+02	1.62991451	0.04524388	2.8	-0.00	12.19716
0.5800E+02	1.62355973	0.04139909	2.5	-0.00	12.36466
0.6000E+02	1.60214676	0.03821128	2.4	-0.00	12.41018
0.6400E+02	1.58807797	0.03367956	2.1	-0.00	12.70462
0.6800E+02	1.52766658	0.03294138	2.2	-0.00	12.59746
0.7200E+02	1.50300776	0.03506735	2.3	-0.00	12.75344
0.7600E+02	1.52951082	0.03779796	2.5	-0.00	13.33397
0.8000E+02	1.50531038	0.03952187	2.6	-0.00	13.46391
0.8400E+02	1.49466433	0.05179046	3.5	-0.00	13.69882
0.8800E+02	1.43642139	0.05050334	3.5	-0.00	13.47483
0.9200E+02	1.40187777	0.05064134	3.6	-0.00	13.44634
0.9600E+02	1.37486499	0.04984519	3.6	-0.00	13.47087
0.1000E+03	1.39795058	0.04978102	3.6	-0.00	13.97951
0.1040E+03	1.35715233	0.04982495	3.7	-0.00	13.84029
0.1080E+03	1.40050950	0.06391168	4.6	-0.00	14.55452
0.1120E+03	1.33838506	0.06028666	4.5	-0.00	14.16414
0.1160E+03	1.36012357	0.06032615	4.4	-0.00	14.64898
0.1200E+03	1.32912261	0.05901155	4.4	-0.00	14.55981
0.1280E+03	1.32326089	0.05640237	4.3	-0.00	14.97099
0.1360E+03	1.30672112	0.05455007	4.2	-0.00	15.23886
0.1440E+03	1.28607932	0.04975196	3.9	-0.00	15.43295
0.1520E+03	1.30942091	0.05474495	4.2	-0.00	16.14363
0.1600E+03	1.30399562	0.05562677	4.3	-0.00	16.49438
0.1680E+03	1.28121748	0.05814145	4.5	-0.00	16.60648
0.1760E+03	1.32355200	0.05811452	4.4	-0.00	17.55890
0.1840E+03	1.32723779	0.06232689	4.7	-0.00	18.00353
0.1920E+03	1.31017685	0.05719415	4.4	-0.00	18.15434
0.2000E+03	1.31812719	0.05706246	4.3	-0.00	18.64113

C Output Files for $^{239}\text{Pu}(\text{n},\text{f})$ Cross Sections

1 RESULT PU9(n,f)

E/MEV	CS/B	DCS/B	DCS/\%	DIF/\%	CS*SQRT(E)
0.2530E-07	752.18874429	2.25989141	0.3	0.00	0.11964
0.1500E-03	18.91820519	0.11596612	0.6	0.00	0.23170
0.2500E-03	18.13576958	0.11800793	0.7	0.00	0.28675
0.3500E-03	8.64878725	0.06317426	0.7	-0.00	0.16180
0.4500E-03	9.70898933	0.06244771	0.6	0.00	0.20596
0.5500E-03	15.67404588	0.11321516	0.7	0.00	0.36759
0.6500E-03	4.60443426	0.03539273	0.8	-0.00	0.11739
0.7500E-03	5.76516116	0.04397126	0.8	-0.00	0.15789
0.8500E-03	5.09457604	0.03564878	0.7	-0.00	0.14853
0.9500E-03	8.43983444	0.06313869	0.7	0.00	0.26013
0.1500E-02	4.56070265	0.03755947	0.8	-0.00	0.17664
0.2500E-02	3.33229272	0.02600036	0.8	0.00	0.16661
0.3500E-02	3.05642913	0.02361327	0.8	0.00	0.18082
0.4500E-02	2.40949097	0.01958576	0.8	0.00	0.16163
0.5500E-02	2.34004949	0.01897580	0.8	-0.00	0.17354
0.6500E-02	2.04649230	0.01967358	1.0	-0.00	0.16499
0.7500E-02	2.09061717	0.01575990	0.8	0.00	0.18105
0.8500E-02	2.23820432	0.01978915	0.9	0.00	0.20635
0.9500E-02	1.91862855	0.01517921	0.8	-0.00	0.18700
0.1500E-01	1.78919981	0.01258495	0.7	0.00	0.21913
0.2000E-01	1.74717428	0.02421763	1.4	0.00	0.24709
0.2400E-01	1.62107778	0.01199032	0.7	0.00	0.25114
0.3000E-01	1.63023974	0.01287544	0.8	-0.00	0.28237
0.4500E-01	1.52943055	0.01108244	0.7	-0.00	0.32444
0.5500E-01	1.54241469	0.01129546	0.7	0.00	0.36173
0.6500E-01	1.56518110	0.01171201	0.7	0.00	0.39904
0.7500E-01	1.55517269	0.01218403	0.8	-0.00	0.42590
0.8500E-01	1.51191530	0.01172667	0.8	0.00	0.44080
0.9500E-01	1.53356513	0.01514478	1.0	0.00	0.47268
0.1000E+00	1.55415613	0.01314253	0.8	0.00	0.49147
0.1200E+00	1.50709371	0.01127633	0.7	0.00	0.52207
0.1500E+00	1.50173436	0.01063391	0.7	0.00	0.58162
0.1700E+00	1.49134048	0.01196698	0.8	0.00	0.61490
0.1800E+00	1.49307595	0.01649816	1.1	0.00	0.63346
0.1900E+00	1.46292990	0.01557232	1.1	0.00	0.63768
0.2000E+00	1.45204657	0.01485659	1.0	0.00	0.64937
0.2100E+00	1.54467594	0.01564578	1.0	0.00	0.70786
0.2200E+00	1.50079013	0.01378032	0.9	0.00	0.70393
0.2300E+00	1.51355862	0.01338548	0.9	0.00	0.72588
0.2400E+00	1.50228597	0.01786741	1.2	0.00	0.73597
0.2450E+00	1.50136609	0.01395623	0.9	-0.00	0.74314
0.2500E+00	1.50424081	0.01469857	1.0	-0.00	0.75212
0.2600E+00	1.51805522	0.01403043	0.9	0.00	0.77406

0.2700E+00	1.51293165	0.01230131	0.8	0.00	0.78614
0.2800E+00	1.56142411	0.01354097	0.9	0.00	0.82623
0.3000E+00	1.53009082	0.01184634	0.8	0.00	0.83807
0.3250E+00	1.54068136	0.01271617	0.8	-0.00	0.87832
0.3500E+00	1.52662338	0.01145949	0.8	-0.00	0.90316
0.3750E+00	1.54884671	0.01258178	0.8	0.00	0.94847
0.4000E+00	1.54963017	0.01246778	0.8	0.00	0.98007
0.4250E+00	1.56393153	0.01466860	0.9	0.00	1.01956
0.4500E+00	1.58090047	0.01300244	0.8	0.00	1.06050
0.4750E+00	1.56871907	0.01335291	0.9	0.00	1.08117
0.5000E+00	1.57664565	0.01171437	0.7	0.00	1.11486
0.5200E+00	1.58114769	0.01375020	0.9	0.00	1.14018
0.5400E+00	1.56915631	0.01174011	0.7	0.00	1.15309
0.5700E+00	1.59169168	0.01313746	0.8	-0.00	1.20170
0.6000E+00	1.59561341	0.01172517	0.7	-0.00	1.23596
0.6500E+00	1.61641442	0.01088127	0.7	-0.00	1.30319
0.7000E+00	1.62413221	0.01124077	0.7	-0.00	1.35885
0.7500E+00	1.69194491	0.01119947	0.7	-0.00	1.46527
0.8000E+00	1.69789320	0.01130219	0.7	-0.00	1.51864
0.8500E+00	1.69308940	0.01165190	0.7	-0.00	1.56095
0.9000E+00	1.67816498	0.01121589	0.7	-0.00	1.59205
0.9400E+00	1.68226171	0.01195559	0.7	-0.00	1.63101
0.9600E+00	1.72621464	0.01299508	0.8	-0.00	1.69134
0.9800E+00	1.71562681	0.01380438	0.8	-0.00	1.69838
0.1000E+01	1.72697562	0.01074119	0.6	-0.00	1.72698
0.1100E+01	1.74450487	0.01047548	0.6	-0.00	1.82965
0.1250E+01	1.84780217	0.01086598	0.6	-0.00	2.06591
0.1400E+01	1.92821306	0.01162472	0.6	-0.00	2.28149
0.1600E+01	1.95081847	0.01143073	0.6	-0.00	2.46761
0.1800E+01	1.95335525	0.01178266	0.6	-0.00	2.62070
0.2000E+01	1.97953359	0.01222098	0.6	-0.00	2.79948
0.2200E+01	1.96400185	0.01216832	0.6	-0.00	2.91309
0.2400E+01	1.92272829	0.01182866	0.6	-0.00	2.97868
0.2600E+01	1.90775167	0.01225203	0.6	-0.00	3.07616
0.2800E+01	1.89058057	0.01321286	0.7	-0.00	3.16355
0.3000E+01	1.85955156	0.01160098	0.6	-0.00	3.22084
0.3600E+01	1.80763391	0.01087870	0.6	-0.00	3.42974
0.4000E+01	1.76716378	0.01074409	0.6	-0.00	3.53433
0.4500E+01	1.74295339	0.01081269	0.6	-0.00	3.69736
0.4700E+01	1.72933614	0.01116136	0.6	-0.00	3.74911
0.5000E+01	1.68627192	0.01032405	0.6	-0.00	3.77062
0.5300E+01	1.67813349	0.01140353	0.7	-0.00	3.86335
0.5500E+01	1.65960776	0.01101403	0.7	-0.00	3.89213
0.5800E+01	1.69261646	0.01226655	0.7	-0.00	4.07636
0.6000E+01	1.76853025	0.01350583	0.8	-0.00	4.33200
0.6200E+01	1.84315654	0.01542548	0.8	-0.00	4.58942
0.6500E+01	1.94473346	0.01514770	0.8	-0.00	4.95812
0.7000E+01	2.08247597	0.01595872	0.8	-0.00	5.50971
0.7500E+01	2.20491791	0.01751830	0.8	-0.00	6.03842
0.7750E+01	2.24283458	0.02005367	0.9	-0.00	6.24379

0.8000E+01	2.29631246	0.01778614	0.8	-0.00	6.49495
0.8500E+01	2.28267538	0.01794886	0.8	-0.00	6.65509
0.9000E+01	2.27575520	0.01791288	0.8	-0.00	6.82727
0.1000E+02	2.26740767	0.01963162	0.9	-0.00	7.17017
0.1100E+02	2.26276497	0.02000221	0.9	-0.00	7.50474
0.1150E+02	2.23727646	0.02172842	1.0	-0.00	7.58697
0.1200E+02	2.25230231	0.02065965	0.9	-0.00	7.80220
0.1300E+02	2.35035865	0.01818505	0.8	-0.00	8.47434
0.1400E+02	2.41689792	0.01609820	0.7	-0.00	9.04320
0.1450E+02	2.39220672	0.01506701	0.6	-0.00	9.10925
0.1500E+02	2.39966305	0.01883556	0.8	-0.00	9.29386
0.1600E+02	2.42697624	0.02199383	0.9	-0.00	9.70790
0.1700E+02	2.35999950	0.02239960	0.9	-0.00	9.73053
0.1800E+02	2.33666289	0.02247703	1.0	-0.00	9.91362
0.1900E+02	2.35315544	0.02043904	0.9	-0.00	10.25717
0.2000E+02	2.35694817	0.02636201	1.1	-0.00	10.54059
0.2100E+02	2.36886928	0.02616013	1.1	-0.00	10.85552
0.2200E+02	2.37110206	0.04113758	1.7	0.00	11.12145
0.2300E+02	2.36910433	0.03174324	1.3	-0.00	11.36183
0.2400E+02	2.29660790	0.03466543	1.5	-0.00	11.25103
0.2500E+02	2.33441940	0.03033960	1.3	-0.00	11.67210
0.2600E+02	2.30661183	0.03678936	1.6	-0.00	11.76146
0.2700E+02	2.31174063	0.03185517	1.4	-0.00	12.01216
0.2800E+02	2.33779072	0.04030484	1.7	-0.00	12.37043
0.2900E+02	2.28074114	0.03172922	1.4	-0.00	12.28217
0.3000E+02	2.34242099	0.03446007	1.5	-0.00	12.82997
0.3200E+02	2.30376634	0.04236377	1.8	-0.00	13.03207
0.3400E+02	2.27698867	0.04199898	1.8	-0.00	13.27701
0.3600E+02	2.18774364	0.04521103	2.1	-0.00	13.12646
0.3800E+02	2.12749190	0.04734418	2.2	-0.00	13.11474
0.4000E+02	2.13665109	0.04864688	2.3	-0.00	13.51337
0.4200E+02	2.10752625	0.04487802	2.1	-0.00	13.65833
0.4400E+02	2.11381097	0.04595785	2.2	-0.00	14.02144
0.4600E+02	2.09882682	0.04302462	2.0	-0.00	14.23494
0.4800E+02	2.06834664	0.05007109	2.4	-0.00	14.32993
0.5000E+02	2.03855681	0.05106239	2.5	-0.00	14.41477
0.5200E+02	2.03589889	0.05614535	2.8	-0.00	14.68108
0.5400E+02	2.00881369	0.05531761	2.8	-0.00	14.76171
0.5600E+02	2.05061377	0.05758821	2.8	-0.00	15.34539
0.5800E+02	2.02246940	0.05219049	2.6	-0.00	15.40267
0.6000E+02	2.00077297	0.04855506	2.4	-0.00	15.49792
0.6400E+02	1.98184264	0.04299636	2.2	-0.00	15.85474
0.6800E+02	1.91400835	0.04183836	2.2	-0.00	15.78332
0.7200E+02	1.87524676	0.04448081	2.4	-0.00	15.91200
0.7600E+02	1.86944706	0.04677179	2.5	-0.00	16.29746
0.8000E+02	1.84138858	0.04927363	2.7	-0.00	16.46988
0.8400E+02	1.84046599	0.06467432	3.5	-0.00	16.86815
0.8800E+02	1.75783806	0.06228610	3.5	-0.00	16.48998
0.9200E+02	1.72433035	0.06268995	3.6	-0.00	16.53920
0.9600E+02	1.70357448	0.06205777	3.6	-0.00	16.69155

0.1000E+03	1.70968564	0.06167498	3.6	-0.00	17.09686
0.1040E+03	1.63051629	0.06086308	3.7	-0.00	16.62807
0.1080E+03	1.68795012	0.07791110	4.6	-0.00	17.54169
0.1120E+03	1.63809841	0.07469042	4.6	-0.00	17.33600
0.1160E+03	1.66195610	0.07425237	4.5	-0.00	17.89982
0.1200E+03	1.59169013	0.07194223	4.5	-0.00	17.43609
0.1280E+03	1.59354689	0.06871473	4.3	-0.00	18.02893
0.1360E+03	1.55935886	0.06539710	4.2	-0.00	18.18509
0.1440E+03	1.53707366	0.06045275	3.9	-0.00	18.44488
0.1520E+03	1.57977184	0.06639968	4.2	-0.00	19.47674
0.1600E+03	1.53207231	0.06628414	4.3	-0.00	19.37935
0.1680E+03	1.53528695	0.07132485	4.6	-0.00	19.89959
0.1760E+03	1.55558254	0.06912566	4.4	-0.00	20.63713
0.1840E+03	1.54297598	0.07278020	4.7	-0.00	20.92994
0.1920E+03	1.51488381	0.06656536	4.4	-0.00	20.99085
0.2000E+03	1.53188888	0.06769341	4.4	-0.00	21.66418

D Comparison between this Evaluation and the LLNL Evaluation from May 2022 Using fissionTPC Data

In Fig. 17, the evaluated $^{239}\text{Pu}(\text{n},\text{f})$ cross sections obtained here are compared to an evaluation by LLNL from May 2022 that also used the FissionTPC data [19]. The latter evaluation differs from the one described here by:

- LLNL evaluators used the GMA code version and database from 2014, i.e., a version of the database and code that was before the 2018 standard that was also included in ENDF/B-VIII.0. However, this is also not the version for the previous standard (included in ENDF/B-VII.0), but in-between those two standard releases,
- Consequently, newest standard changes starting from 2018 are missing as well. This includes updates to ^{239}Pu experimental covariances using templates of expected measurement uncertainties [13]. While it is stated in Ref. [19] that the impact is minimal, it was shown in Ref. [13] that the change in the $^{239}\text{Pu}(\text{n},\text{f})$ cross sections due to templates of expected measurement uncertainties leads to a drop of 90 pcm in k_{eff} of Jezebel,
- FissionTPC covariances were not considered.

Given the many changes since the 2014 GMA code and database version, it is hard to find one distinct reason for the differences in the $^{239}\text{Pu}(\text{n},\text{f})$ cross section, but it is obvious that they are large from 8–12 MeV and distinct from 300–600 keV.

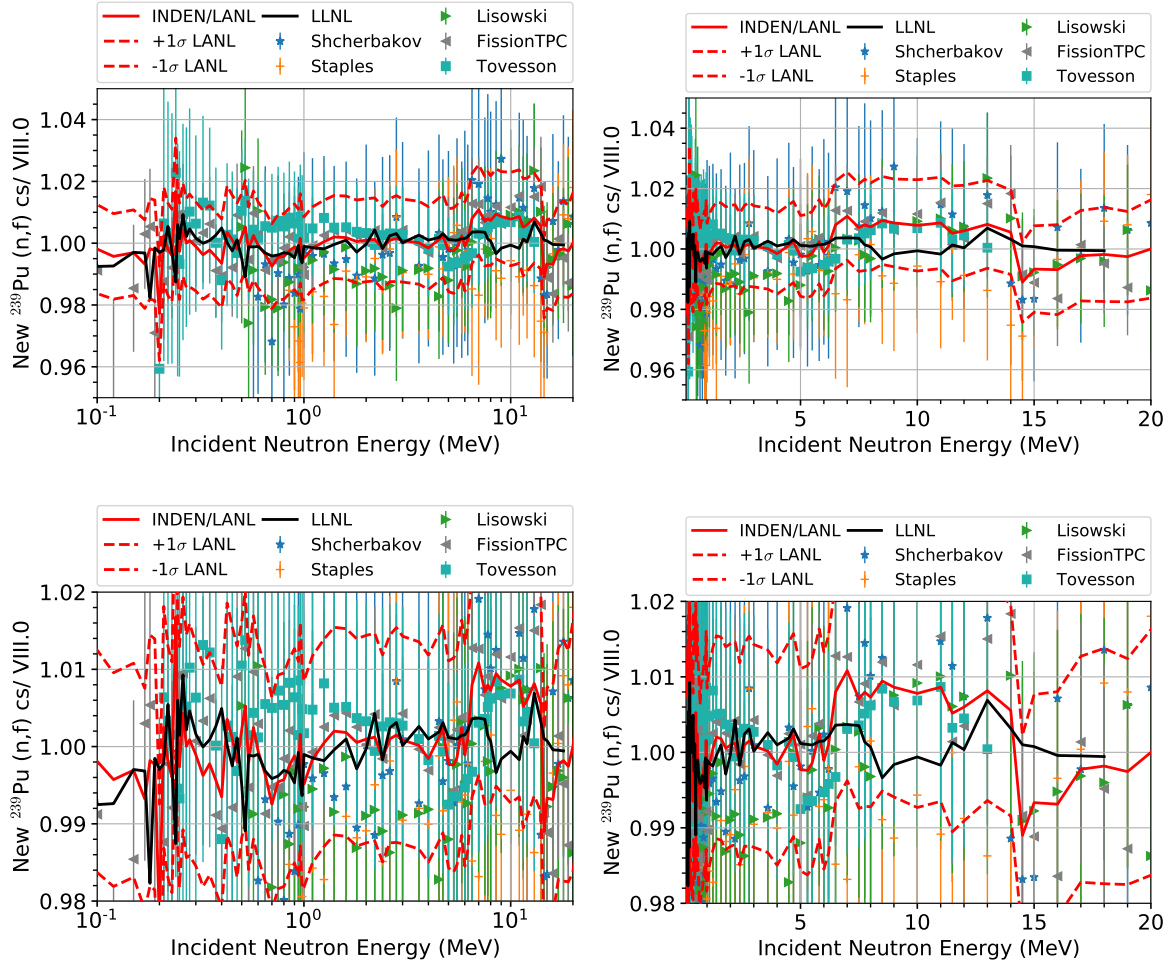


Figure 17: Comparison of this $^{239}\text{Pu}(n,f)$ cross section evaluation to one by LLNL from May 2022 using FissionTPC data [19].